catalysts

MDPI

Article

Analysis and Model-Based Description of the Total Process of Periodic Deactivation and Regeneration of a VO_x Catalyst for Selective Dehydrogenation of Propane

Andreas Brune [1,2,*], Andreas Seidel-Morgenstern [1] and Christof Hamel [1,2,*]

[1] Institute of Process Engineering, Otto von Guericke University Magdeburg, Universitätsplatz 2, 39106 Magdeburg, Germany; anseidel@ovgu.de
[2] Process Engineering, Anhalt University of Applied Sciences, Bernburger Straße 55, 06354 Köthen, Germany
* Correspondence: andreas.brune@ovgu.de (A.B.); christof.hamel@hs-anhalt.de (C.H.)

Received: 26 October 2020; Accepted: 22 November 2020; Published: 25 November 2020

Abstract: This study intends to provide insights into various aspects related to the reaction kinetics of the VO_x catalyzed propane dehydrogenation including main and side reactions and, in particular, catalyst deactivation and regeneration, which can be hardly found in combination in current literature. To kinetically describe the complex reaction network, a reduced model was fitted to lab scale experiments performed in a fixed bed reactor. Additionally, thermogravimetric analysis (TGA) was applied to investigate the coking behavior of the catalyst under defined conditions considering propane and propene as precursors for coke formation. Propene was identified to be the main coke precursor, which agrees with results of experiments using a segmented fixed bed reactor (FBR). A mechanistic multilayer-monolayer coke growth model was developed to mathematically describe the catalyst coking. Samples from long-term deactivation experiments in an FBR were used for regeneration experiments with oxygen to gasify the coke deposits in a TGA. A power law approach was able to describe the regeneration behavior well. Finally, the results of periodic experiments consisting of several deactivation and regeneration cycles verified the long-term stability of the catalyst and confirmed the validity of the derived and parametrized kinetic models for deactivation and regeneration, which will allow model-based process development and optimization.

Keywords: deactivation; coking; regeneration; propane dehydrogenation; VO_x catalyst; periodic operation; kinetic modeling; reaction kinetics

1. Introduction

Light olefins are some of the most important building blocks in the chemical industry [1]. Most of the light olefins are currently produced by highly optimized steam cracking processes. Since feedstocks are shifting progressively toward light alkanes, on-purpose technologies for the production of propene and other short chain alkenes have drawn more and more attention and are still considered in research [2–5]. Dehydrogenation of propane is a well-known alternative production route for producing propene that was already commercialized [6]. Besides being energy intensive, the catalysts used in these processes are known to suffer from rapid coking, which requires periodic regeneration. Furthermore, the endothermic thermal dehydrogenation reaction itself is limited by a chemical equilibrium.

Examples illustrating how industry faces these drawbacks are found with the Catofin and Oleflex processes, among others (Figure 1). In the Catofin process, several adiabatic fixed bed reactors are used in parallel to ensure a semi-continuous production of propene. Each reactor is used for dehydrogenation

(Figure 1a) for around 10 min followed by a regeneration period (Figure 1b) of roughly 10 min (see Figure 2) [7]. Between the dehydrogenation and the regeneration phase, the reactors have to be purged and evacuated. Regeneration and production phases are scheduled to ensure a constant product flow. During the production phase the catalyst loses activity due to coking and the temperature of the reactor decreases due to the endothermic reaction. During the regeneration phase hot air is used to restore the activity by burning the coke and to heat up the reactor again. It has to be noted that a continuous production can only be realized by applying simultaneously several reactors due to the tremendous downtimes of each individual reactor.

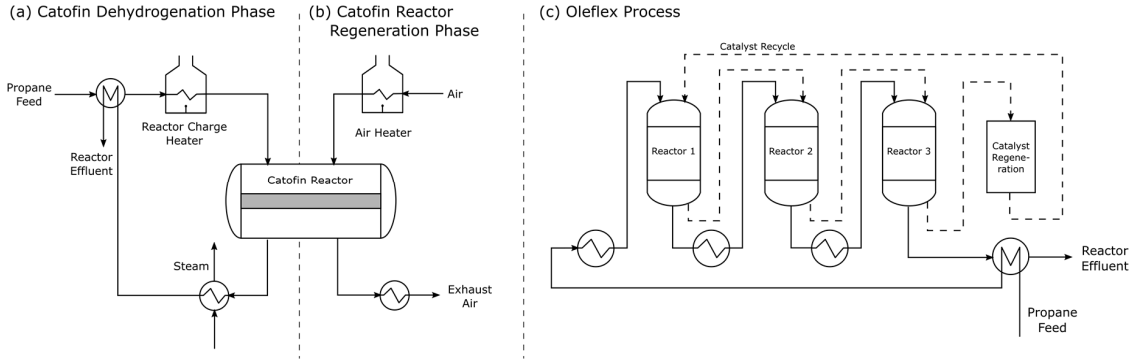

Figure 1. Simplified flow sheets of commercialized dehydrogenation processes: (**a**) Catofin process during production phase, (**b**) Catofin process during regeneration phase, (**c**) Oleflex process [6–8].

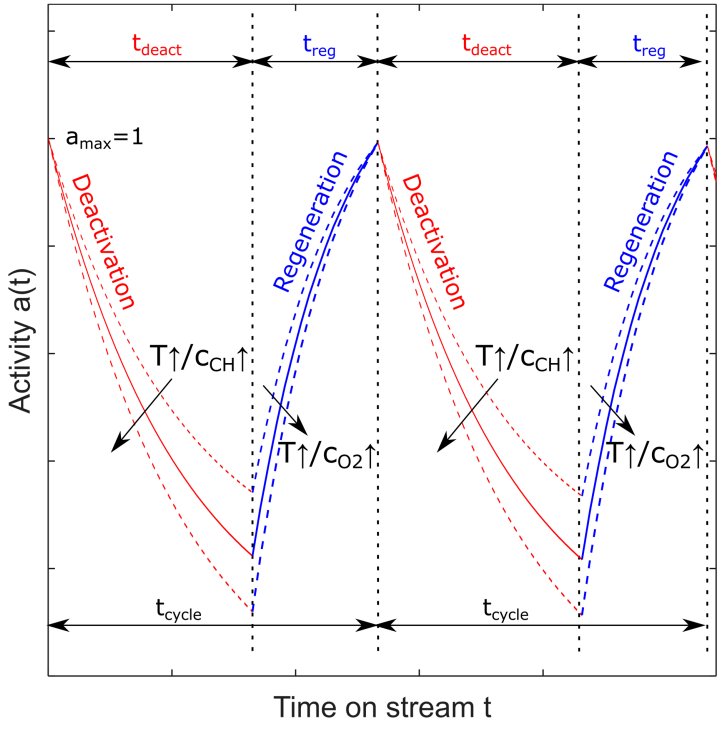

Figure 2. Schematic of periodic operation of a reactor switching between deactivation and regeneration phases.

The Oleflex process uses three moving bed radial flow reactors in series (Figure 1c). It deals with the endothermicity of the process by heating up the gas flow with interstage heaters after each reactor. The catalyst leaving the third reactor is fed to a regeneration unit to restore the initial activity by gasification of coke. The regenerated catalyst is recycled to the first reactor and is moved in the same direction as the gas to the next reactor [8]. This process needs a more complex reactor setup and

places high demands on the catalyst which has to be mechanically stable to be used in a moving bed reactor. Besides that it is not possible to remove coke built up on the reactor surfaces or the devices in the reactor during operation [6].

Thus, process intensification is needed to overcome some disadvantages of the established plant designs and can lead to a more sustainable and energy effective overall process [9]. Numerous research activities in the field of process intensification are related to membrane reactors [10,11]. Membrane reactors can provide distribution or extraction of intermediates, reactants, or products to assure a more advantages concentration and temperature regime than conventional reactor designs [12]. Porous and dense membranes are subject of current research [13,14].

Different membrane reactors were already used for the dehydrogenation of short chain alkanes [15–22]. Coking of the catalyst used in membrane reactors as well as coking of the membranes themselves was repeatedly reported [11,19–21,23]. Various reactor setups and strategies able to prevent coking or regenerate the coked catalyst were also suggested [15,23]. A new innovative approach can be the application of periodic regeneration in a membrane reactor in distributor configuration coupling thermal and oxidative dehydrogenation in one apparatus [15]. This concept avoids downtimes due to the operando regeneration of the catalyst as in established processes discussed above. Coupling of the exothermic oxidative dehydrogenation and the endothermic thermal dehydrogenation can lead to an autothermic operation and improves energy efficiency.

To be able to evaluate the possibilities of periodic regeneration of the catalyst a profound knowledge of the reaction network is needed. This includes parallel and side reactions as well as deactivation and regeneration of the catalyst which occurs simultaneously. A combined study of all relevant effects with a systematic model discrimination is rarely found in the literature.

In this contribution the reaction network of the dehydrogenation of propane on a vanadium oxide (VO_x) catalyst is investigated and modeled. The main and side reactions are studied in a lab scale fixed bed reactor and the kinetics are described by a power law approach. The coking behavior and regeneration of the catalyst are studied in a setup for thermogravimetric analysis (TGA), equipped with mass flow controllers (MFCs) for dosing of propane, propene, O_2 and N_2. For describing the coking of the catalyst, different multilayer-monolayer coke growth models (MMCGM) with different reaction orders are further developed and tested. It is shown that it is possible to describe the regeneration kinetics by a reduced model. Deactivation and regeneration kinetics as well as long-term stability of the catalyst are validated by periodic experiments including deactivation and regeneration phases in several subsequent cycles as illustrated in Figure 2 and occurring in commercialized industrial processes as discussed above.

2. Results and Discussion

This chapter presents the results of the kinetic analysis of the reaction network first (Section 2.1). After that the findings of kinetic modeling and parametrization of the catalyst coking are explained and discussed (Section 2.2), followed by an analysis of the regeneration kinetics (Section 2.3). Afterwards the deactivation and the regeneration models are validated by periodic experiments (Section 2.4).

2.1. Kinetic Investigation of the Reaction Network

For all experiments in this study a VO_x catalyst was used [15–18]. Kinetic experiments were conducted in a lab scale tubular fixed bed quartz glass reactor, which is described in detail in the Materials and Methods section of this contribution. Isothermal conditions and plug flow were assumed.

Figure 3 shows the reaction network postulated for the coupled thermal and oxidative dehydrogenation of propane on VO_x. Commercialized processes (Oleflex, Catofin, etc.) are currently based on the thermal dehydrogenation (TDH, R_1, Equation (1)) with the major drawback of rapid catalyst coking and is furthermore limited by a thermodynamic equilibrium [6].

$$R_1: \quad C_3H_8 \rightleftharpoons C_3H_6 + H_2 \tag{1}$$

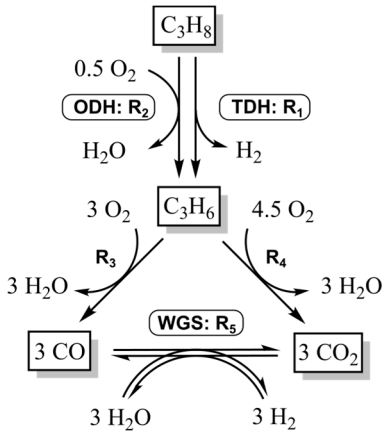

Figure 3. Reaction network of the dehydrogenation of propane on a VO_x catalyst.

A promising alternative is the oxidative dehydrogenation (ODH, R_2, Equation (2)).

$$R_2: \quad C_3H_8 + 0.5\,O_2 \rightarrow C_3H_6 + H_2O \tag{2}$$

The oxygen needed for the ODH largely prevents coking but decreases the selectivity due to unwanted consecutive reactions namely series and total oxidation of the desired product propene (R_3, R_4). Reaction R_5 describes the water–gas shift reaction, which has shown to be beneficial for overcoming the chemical equilibrium of the TDH by consuming the hydrogen produced in the TDH [15].

For a mathematical description of the reaction network a power law approach was used and extended (Equations (3)–(7))

$$r_1 = k_1 \cdot p_{C_3H_8}^{a_1} \tag{3}$$

$$r_2 = k_2 \cdot p_{C_3H_8}^{a_2} \cdot p_{O_2}^{b_2} \tag{4}$$

$$r_3 = k_3 \cdot p_{C_3H_6}^{a_3} \cdot p_{O_2}^{b_3} \tag{5}$$

$$r_4 = k_4 \cdot p_{C_3H_6}^{a_4} \cdot p_{O_2}^{b_4} \tag{6}$$

$$r_5 = k_5 \cdot p_{H_2} \cdot p_{CO_2} \cdot \left(1 - \frac{p_{H_2O} \cdot p_{CO}}{\frac{1}{K_{WGS}} \cdot p_{H_2} \cdot p_{CO_2}}\right) \tag{7}$$

p_i represents the partial pressure of component i, a_i is the reaction order with respect to propane and propene and b_i is the reaction order of oxygen. K_{WGS} represents the equilibrium constant of the water–gas shift reaction (Equation (8)) [24]:

$$K_{WGS} = 1.767 \times 10^{-2} \cdot \exp\left(\frac{4400}{T}\right) \tag{8}$$

The temperature dependency of this model was described by a reparametrized Arrhenius approach (Equations (9)–(11), $T_{ref} = 450\ ^\circ C$)

$$A_j = \ln\left(k_{0,j}\right) - \frac{E_{A,j}}{R\,T_{ref}} \tag{9}$$

$$B_j = \frac{E_{A,j}}{R\,T_{ref}} \tag{10}$$

$$k_j = \exp\left[A_j + B_j\left(\frac{T - T_{ref}}{T}\right)\right] \tag{11}$$

This approach minimizes the correlation between the activation energy E_A and the collision factor k of the standard Arrhenius equation (Equation (12)) [25].

$$k_j = k_{0,j} \exp\left[\frac{E_{A,j}}{R\,T}\right] \tag{12}$$

Details about the parameter estimation are given in the Materials and Methods Section 3.2. Figure 4 reveals the parity plot of the optimized parameters and the experimental data and shows that the simulated data are in good agreement with the experimental data. The estimated parameters are summarized in the Supplementary Material (Tables S1 and S2). It has to be mentioned that the kinetic parameters of the water–gas shift reaction are of less influence. Therefore, it is reasonable to simplify the network. Furthermore, the small reaction order of oxygen of the ODH reaction is notable.

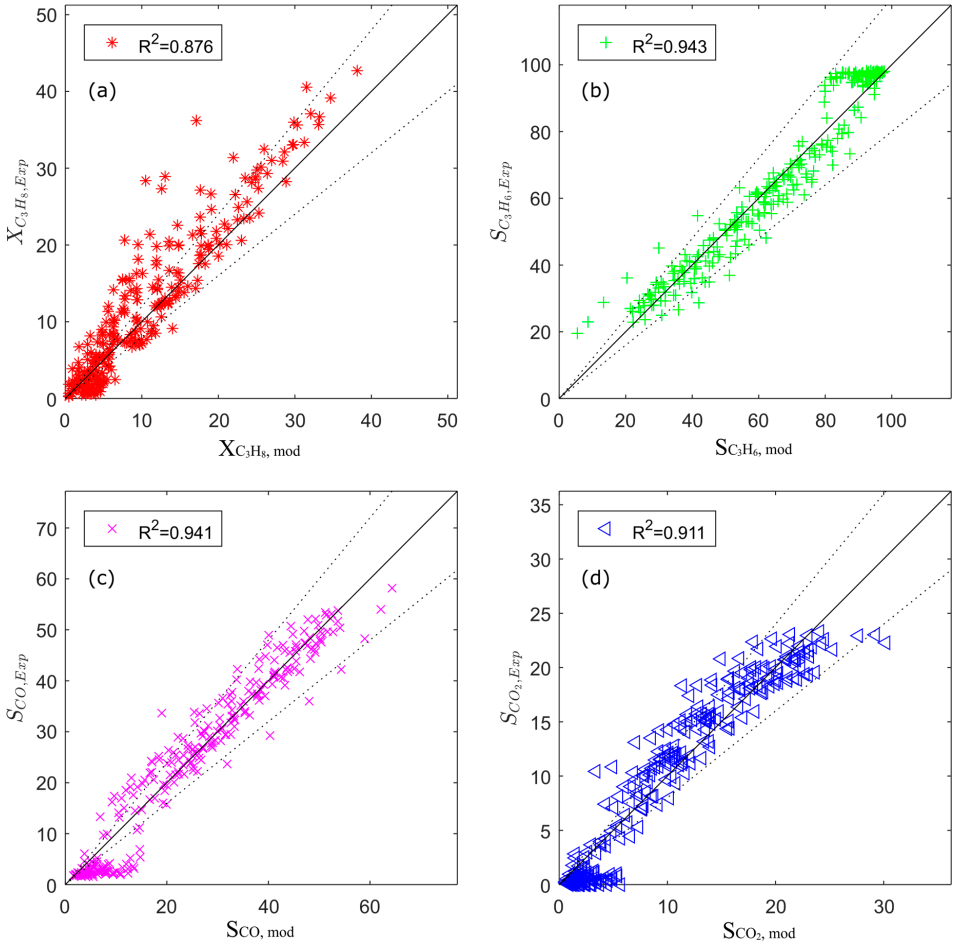

Figure 4. Parity plots for the estimated kinetic model: (**a**) conversion of propane; (**b**) selectivity of propene; (**c**) selectivity of CO; (**d**) selectivity of CO_2.

Nevertheless, the derived kinetic equations are able to describe the reaction network over a wide range of temperatures, oxygen, and propane concentrations. However, deactivation effects are not considered yet. It is well-known that under oxygen lean conditions catalysts tend to deactivate over time due to coking [26]. These coke deposits are responsible for a loss of catalyst activity. The next chapter will present the results of coking experiments and mechanistic mathematical modeling to describe this phenomenon.

2.2. Catalyst Deactivation

Coking experiments were conducted in a TGA setup (see Materials and Methods Section 3.3) that allows deactivating the catalyst at constant temperature in a defined gas atmosphere adjusted by MFCs. The TGA is coupled with a Micro GC for a fast online analysis of gas compositions. Propene and propane were used as coking precursors. Preliminary experiments showed that experiments with temperatures between 575 °C and 650 °C offer a reasonable deactivation behavior at simultaneously high reactor performance. The temperature was varied in steps of 25 K within these limits between the experiments. The mass change and catalyst temperature were recorded by the TGA during the experiments. All studied deactivation experiments are summarized in Table 11 (see Materials and Methods Section 3.3).

A comparison between the coking behavior of the catalyst at different temperatures and between propane and propene feeds is illustrated in Figure 5a. Propene is more reactive than propane, therefore propene is characterized as the dominant coke precursor [26]. For both reactants the coke built up is faster at higher temperatures (Figure 5a). Figure 5b shows that the coking rate increases with increasing propane concentration and also more significantly for increasing propene concentration.

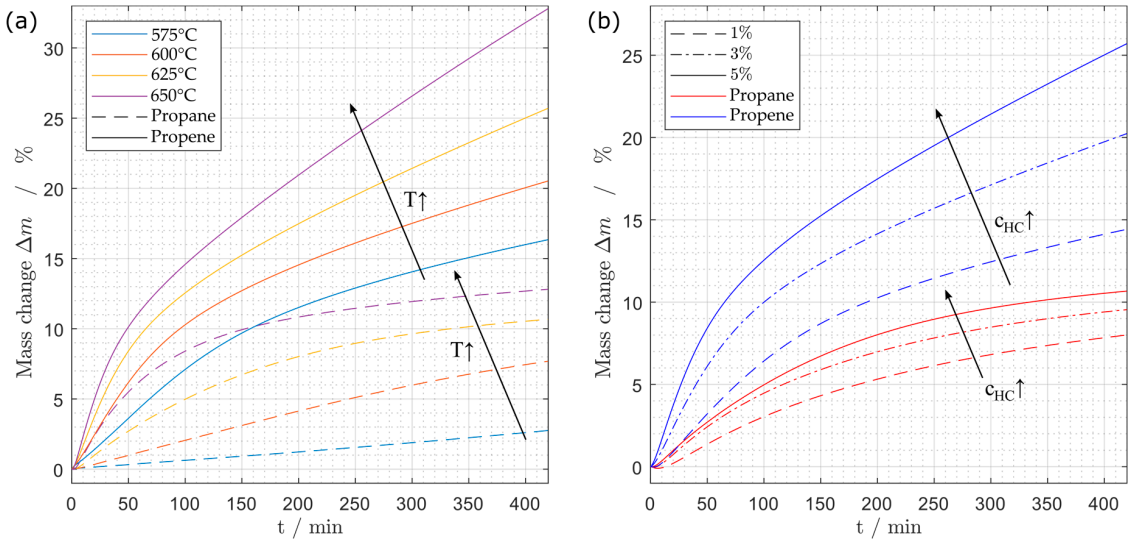

Figure 5. Comparison of the coking behavior of the catalyst using different precursors at (**a**) different temperatures and a concentration of 5% of propane or propene respectively and (**b**) a temperature of 625 °C and varying hydrocarbon concentrations.

Furthermore, it is possible to observe a decrease in sample mass at the beginning of the measurement. Directly after starting the measurement the catalyst loses weight (see Figure 6). This behavior depends on the temperature and was described in detail by Sokolov et al. for other VO_x catalysts [27]. The reason for this counter intuitive mass loss is the desorption of water and the partial reduction of the vanadium oxide of the catalyst since lattice oxygen is consumed during the dehydrogenation reaction, which is an additional aspect that has to be implemented in the kinetic model. The analytical methods use do not allow distinguishing between mass loss to desorption and mass loss due to partial oxidation and this observation can therefore only be described phenomenologically. It cannot be observed for measurements with propene because the rapid increase in mass due to coking compared to propane overlays these effects.

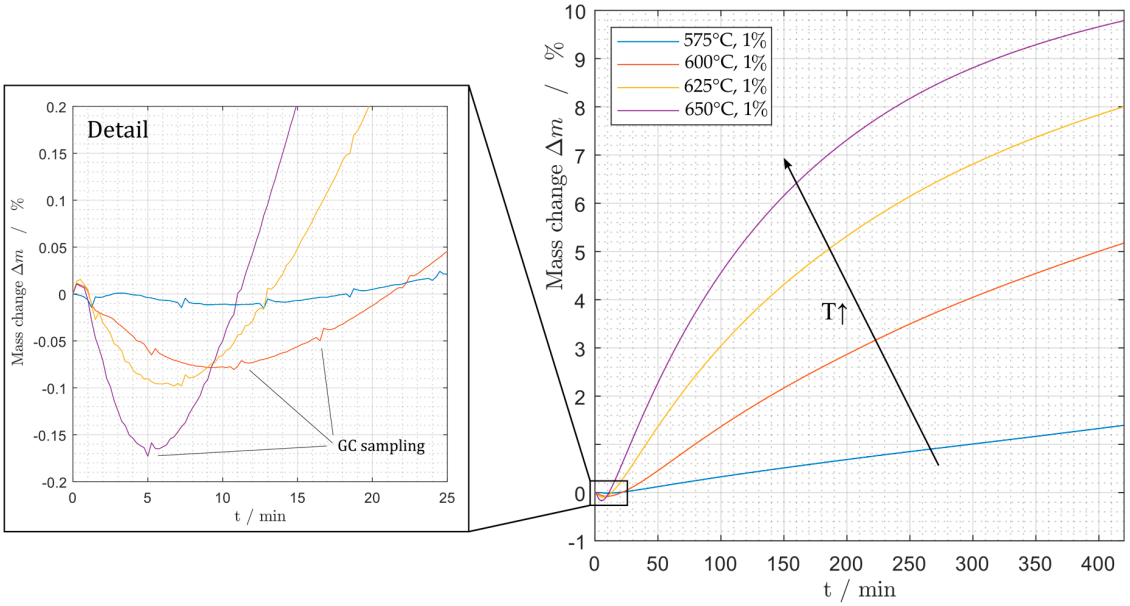

Figure 6. Mass change during deactivation at different temperatures and 1% propane.

In Figure 6 it is also visible that the sampling of the GC caused defined but neglectable disturbances, which did not affect the quality of the measured data.

To be able to evaluate the time for regeneration it is inevitable to describe the catalyst coking by a mathematical model. In this contribution the multilayer-monolayer coke growth model (MMCGM) was used [28]. It is assumed that total amount of coke that is built up on the catalyst surface is either formed as a monolayer (c_m) or as a multilayer (c_M). The total amount of coke is described as the addition of both terms (Equations (13) and (14)).

$$c = c_m + c_M \tag{13}$$

$$r_c = \frac{dc_c}{dt} = \frac{dc_m}{dt} + \frac{dc_M}{dt} \tag{14}$$

The coking rate of the monolayer and for the multilayer can be described by Equation (15) and Equation (16), respectively.

$$r_{c_m} = \frac{dc_m}{dt} = k_m \cdot (c_{max} - c_m)^h \tag{15}$$

$$r_{c_M} = \frac{dc_M}{dt} = k_M \cdot c_m^n \cdot (c_{max} - c_m)^m \tag{16}$$

c_{max} is the maximum coke concentration of the monolayer, h describes the reaction order of the monolayer coke growth and m and n the reaction orders of the multilayer coke growth, respectively. The rate constants of the monolayer and multilayer coke growth k_m and k_M are given by a standard Arrhenius approach (Equation (12), $j \in \{m, M\}$).

Different reaction orders were tested in the literature to describe the coke growth on different catalysts [28]. Table 1 summarizes different integrated forms of the MMCGM known from literature that were tested in this contribution (A1, B1, D1). Besides the forms known from literature an additional approach using a free parameter for the reaction order h of the monolayer was developed (C1, Equation (19)).

Table 1. Integrated form of the multilayer-monolayer coke growth model (MMCGM, Equations (14)–(16)) for different reaction orders.

(A1)	$h = 1$	$n = 0$	$m = 0$	$c = c_{max} \cdot \left(1 - e^{-k_m \cdot t}\right) + k_m \cdot t$	(17)
(B1)	$h = 2$	$n = 0$	$m = 0$	$c = \frac{k_m \cdot t \cdot {c_{max}}^2}{k_m \cdot t \cdot c_{max} + 1} + k_M \cdot t$	(18)
(C1) [1]	$h = h$	$n = 0$	$m = 0$	$c = c_{max} - \left((h-1) \cdot k_m \cdot t + {c_{max}}^{1-h}\right)^{\frac{1}{1-h}} + k_M \cdot t$	(19)
(D1)	$h = 1$	$n = 1$	$m = 0$	$c = c_{max} \cdot \left(1 - e^{-k_m \cdot t}\right) \cdot \left[\frac{k_m - k_M}{k_m}\right] + k_M \cdot c_{max} \cdot t$	(20)

[1] Reaction order h is treated as an additional free parameter during parameter estimation.

Since these forms do not take the concentration of the coke precursor c_{HC} into account, the monolayer terms of the models (A1), (B1), (C1) and (D1) were extended by the concentration of the precursor c_{HC} and an exponent l (Equation (21))

$$\frac{dc_m}{dt} = k_m \cdot c_{HC}^{l} \cdot (c_{max} - c_m) \tag{21}$$

The integrated rate laws following from this new developed extended approach are listed in Table 2.

Table 2. Integrated form of the multilayer-monolayer coke growth model (MMCGM, Equations (14), (16) and (21)) for different reaction orders extended by a precursor concentration dependent term.

(A2)	$h = 1$	$n = 0$	$m = 0$	$c = c_{max} \cdot \left(1 - e^{-k_m \cdot c_{HC}^{l} \cdot t}\right) + k_M \cdot t$	(22)
(B2)	$h = 2$	$n = 0$	$m = 0$	$c = \frac{k_m \cdot c_{HC}^{l} \cdot t \cdot {c_{max}}^2}{k_m \cdot c_{HC}^{l} \cdot t \cdot c_{max} + 1} + k_M \cdot t$	(23)
(C2) [1]	$h = h$	$n = 0$	$m = 0$	$c = c_{max} - \left((h-1) \cdot k_m \cdot c_{HC}^{l} \cdot t + {c_{max}}^{1-h}\right)^{\frac{1}{1-h}} + k_M \cdot t$	(24)
(D2)	$h = 1$	$n = 1$	$m = 0$	$c = c_{max} \cdot \left(1 - e^{-k_m \cdot c_{HC}^{l} \cdot t}\right) \cdot \left[\frac{k_m \cdot c_{HC}^{l} - k_M}{k_m \cdot c_{HC}^{l}}\right] + k_M \cdot c_{max} \cdot t$	(25)

[1] Reaction order h is treated as an additional free parameter during parameter estimation.

For the kinetic analysis of the catalyst coking it was assumed that the TGA setup is perfectly mixed and that there are no concentration gradients in the catalyst sample tray. Propene is therefore available in excess and the concentration of propene is assumed to be constant.

2.2.1. Propene as Coke Precursor

The models (A2), (B2), (C2) and (D2) were fitted to the experiments that were using propene as the coke precursor performing the procedure described in the Materials and Methods Section 3.3 (Figure 7). The compared models are not able to describe the curvature of the curve at the beginning of the measurements especially at low temperatures and low concentrations of propane. At higher temperatures and high concentrations, the experiments reveal a linear increase in mass at the end of the deactivation time. The linear multilayer term of the models should be able to describe this behavior. It is clearly visible that model (A2) describes the coking behavior not as precise as the other models. Thus, model (A2) is not suitable as a coking model. To find the most reasonable model, different measures describing the quality were used in the following.

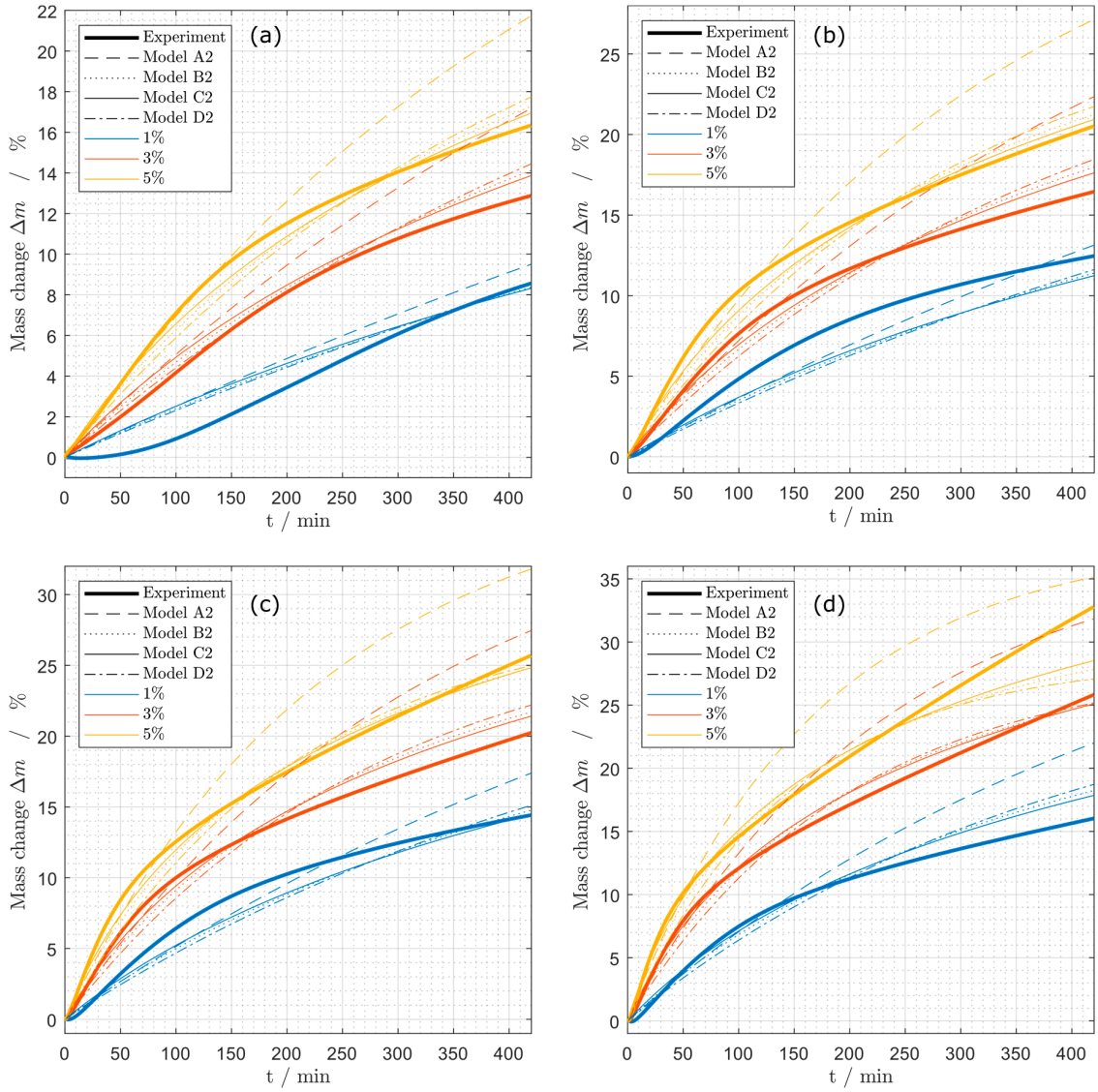

Figure 7. Mass change during coking experiments at different propene concentrations (1%, 3%, 5%) at (**a**) 575 °C, (**b**) 600 °C, (**c**) 625 °C and (**d**) 650 °C for the models (A2), (B2), (C2) and (D2).

A frequently used parameter of validity of a model is the coefficient of determination R^2, which is inadequate for nonlinear regressions [29]. An alternative parameter that can be derived from information theory is the Akaike information criterion (*AIC*), which can be adapted for least squares parameter estimations [30,31]. *AIC* includes the number of model parameters p as well as the residual sum of squares (RSS) and can therefore be used to avoid over-parametrization. For the comparison of different models, it is for reasons of clarity useful to calculate Akaike weights ($w(AIC)$) based on the *AIC* values. These values can be interpreted as the weight of evidence of the model to describe the underlying mechanism among the set of models analyzed (for more information see Supplementary Material, parts B–C). It has to be noted that the AIC is usually only used for independent experimental data, due to the strong correlation of the data. Nevertheless, it is exploited as a measure for qualitative comparison in this contribution. The results of the different evaluation criteria are summed up in Table 3. Model (C2) is according to the evaluation criteria able to describe the experimental data best since it shows the lowest value of the RSS and has the highest Akaike weight regardless of its additional parameter in comparison to the other models tested.

Table 3. Information criteria and comparison of the models (A2), (B2), (C2) and (D2) for deactivation experiments using propene.

-	A2	B2	C2	D2
RSS_{opt}	31,483	22,259	17,241	31,483
p	6	6	7	6
AIC	66,209.7	59,220.4	54,072.2	66,209.7
$w(AIC)$	0.00%	0.00%	100.00%	0.00%

Based on model (C2) different modifications, extensions as well as reductions were tested to achieve a better agreement with the measured data. To study the influence of the multilayer term on the overall mass change, a model consisting only of the monolayer term (model (C3)) was examined.

$$(C3): \quad c = c_{max} - \left((h-1)\cdot k_m \cdot c_{HC}^{l} \cdot t + {c_{max}}^{1-h}\right)^{\frac{1}{1-h}} \tag{26}$$

To be able to describe the mass loss due to desorption at the beginning of the measurements the models (C2) and (C3) were extended by a desorption term (Equations (27) and (28)) [27]. The adsorption term is not depending on temperature, meaning that k_{des} is a constant value for all measurements. A temperature depended desorption term was also tested in preliminary parameter estimations but did not offer any advantages.

$$(C4): \quad c = c_{max} - \left((h-1)\cdot k_m \cdot c_{HC}^{l} \cdot t + {c_{max}}^{1-h}\right)^{\frac{1}{1-h}} + k_M \cdot t - c_0 \cdot \left(1 - e^{-k_{des}\cdot t}\right) \tag{27}$$

$$(C5): \quad c = c_{max} - \left((h-1)\cdot k_m \cdot c_{HC}^{l} \cdot t + {c_{max}}^{1-h}\right)^{\frac{1}{1-h}} - c_0 \cdot \left(1 - e^{-k_{des}\cdot t}\right) \tag{28}$$

Models (C2), (C3), (C4) and (C5) were fitted to the experimental data. The resulting modeled mass changes of the fresh catalyst are summarized in Figure 8.

The plots of the fitted and experimental data depict no visible differences between the models. Table 4 reveals that the residual sum of squares for the optimized models RSS_{opt} show only minor differences. Since the Akaike weight of model (C3) is the highest, this model was finally chosen for describing the coking behavior of the catalyst. The analysis exposes that the multilayer term is not necessary to describe the coking behavior for the experimental conditions tested with the VO_x catalyst and can be neglected for the mathematical modeling of these experiments. The desorption term studied in model (C4) and (C5) has no significant influence on the goodness of fit and can also be disregarded.

Table 4. Information criteria and comparison of the models (C2), (C3), (C4) and (C5) for deactivation using propene.

-	C2	C3	C4	C5
RSS_{opt}	17,240.8	17,164.9	17,166.9	17,166.7
p	7	5	9	7
AIC	54,072	53,979	53,990	53,985
$w(AIC)$	0.00%	95.19%	0.52%	4.29%

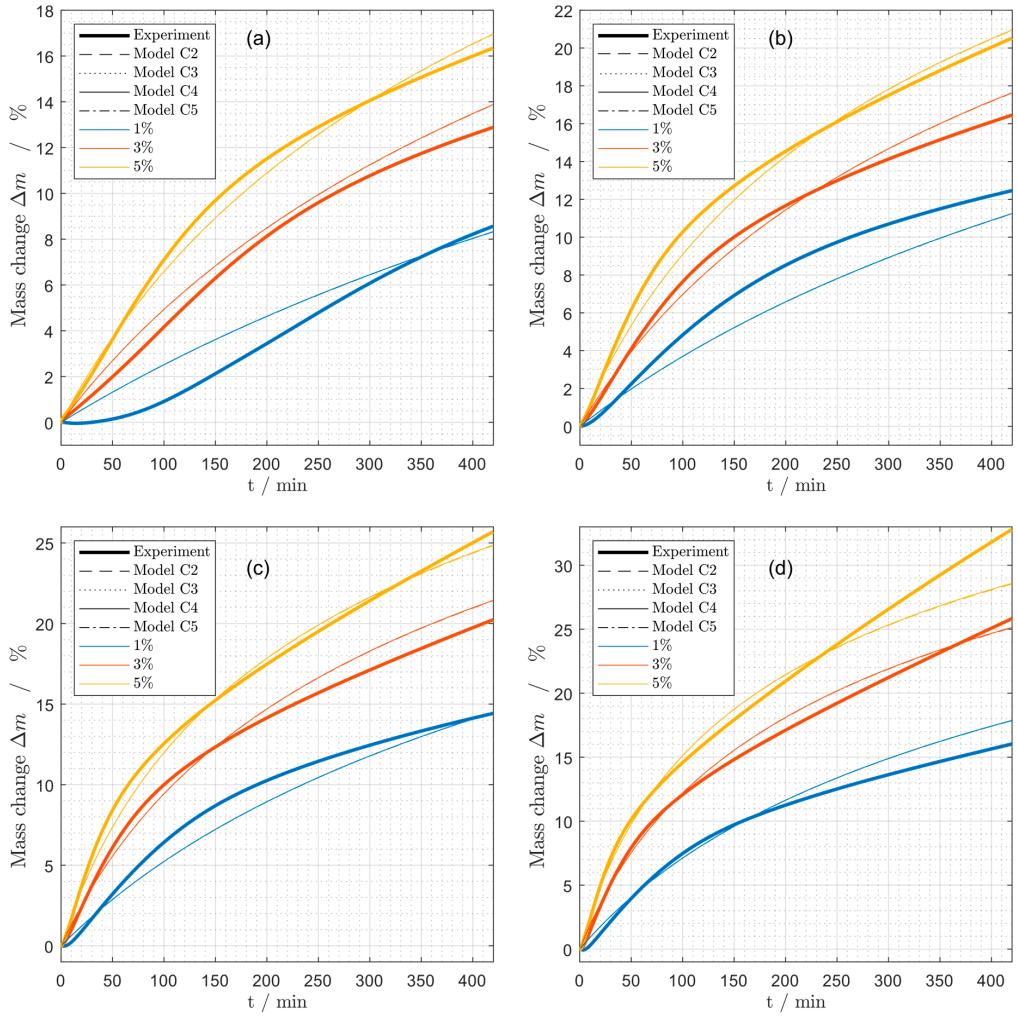

Figure 8. Mass change during coking experiments at different propene concentrations (1%, 3%, 5%) at (**a**) 575 °C, (**b**) 600 °C, (**c**) 625 °C and (**d**) 650 °C for the models (C2), (C3), (C4) and (C5).

Consequently, the reduced model consisting only of a monolayer term (model (C3)) is sufficient to describe the mass changes in the experiments. It has to be stressed that the prediction quality of this model decreases for low concentrations and low temperatures.

The optimized parameters of the selected model are shown in Table 5. For the estimation of confidence intervals (CI) a more suitable bootstrapping algorithm [32–34] was used (see Supplementary Material, parts B–C).

Table 5. Optimized parameters of model C3 to describe the coking behavior of the VO_x catalyst.

Parameter	Opt. Value	Confidence Intervals		Unit
c_{max}	87.060	−0.45%	+0.82%	$\% \left(\frac{kg_{coke}}{kg_{cat}} \times 100\right)$
l	0.700	−0.30%	+0.30%	-
k_0	9.52×10^7	−33.21%	+11.26%	$\left(kg_{coke} kg_{cat}^{-1} \, min^{-1}\right)^{1-h}$
E_A	106,397	−0.13%	+0.12%	$J \, mol^{-1}$
h	6.401	−0.38%	+1.27%	-

2.2.2. Propane as Coke Precursor

Besides describing the deactivation based on propene in the feed, a kinetic analysis of the experiments using propane was also executed. The parameter estimation was performed in the same

way as discussed for propene. A comparison between the unmodified MMCGM models (A2), (B2), (C2), and (D2) is shown in Figure 9.

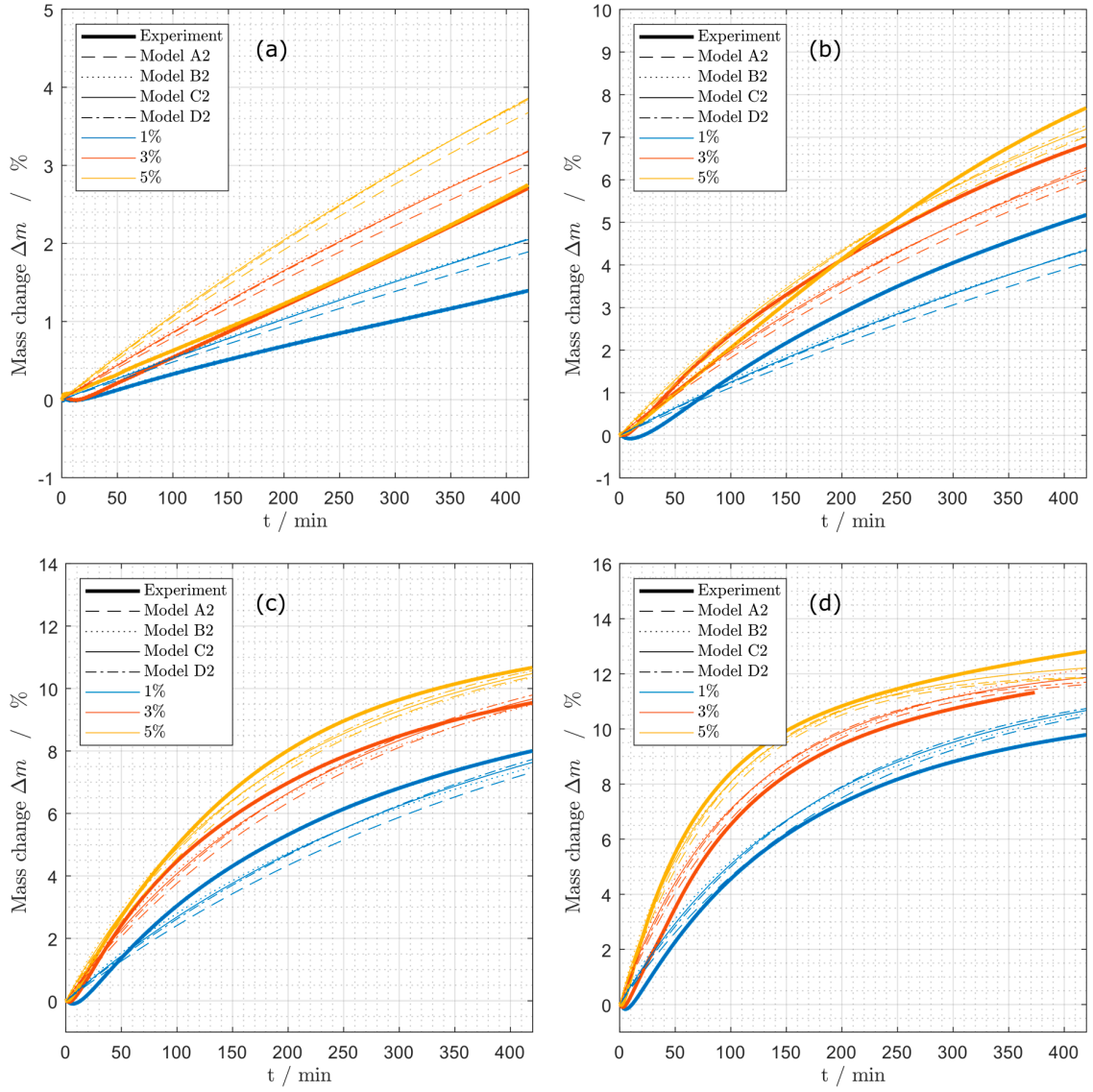

Figure 9. Mass change during coking experiments at different propane concentrations (1%, 3%, 5%) at (**a**) 575 °C, (**b**) 600 °C, (**c**) 625 °C and (**d**) 650 °C for the models (A2), (B2), (C2) and (D2) as used for coking from propene (Table 2).

By comparing the information criteria listed in Table 6, it becomes clear that model (C2) describes the deactivation best.

Table 6. Information criteria and comparison of the models (A2), (B2), (C2) and (D2) for the deactivation of VO_x catalyst with propane.

-	A2	B2	C2	D2
RSS_{opt}	4889.5	5078.9	4783.5	4889.4
p	6	6	7	6
AIC	28,665	29,431	28,225	28,664
$w(AIC)$	0.00%	0.00%	100.00%	0.00%

As well as for the deactivation measurements with propene, the developed models (C3), (C4) and (C5) were compared to model (C2). The corresponding graphs are illustrated in Figure 10. In comparison to the models for the deactivation experiments with propene (Figure 8) there are visible differences between the models. Especially the models including a desorption term ((C4) and (C5)) fit the experimental data at low temperatures and low propane concentrations better than the models without desorption terms. These differences are also evident in the parameters summarized in Table 7. Model (C4) and (C5) show a lower RSS_{opt} value than the other models. Since model (C5) needs two parameters less than model (C4) it is to be preferred.

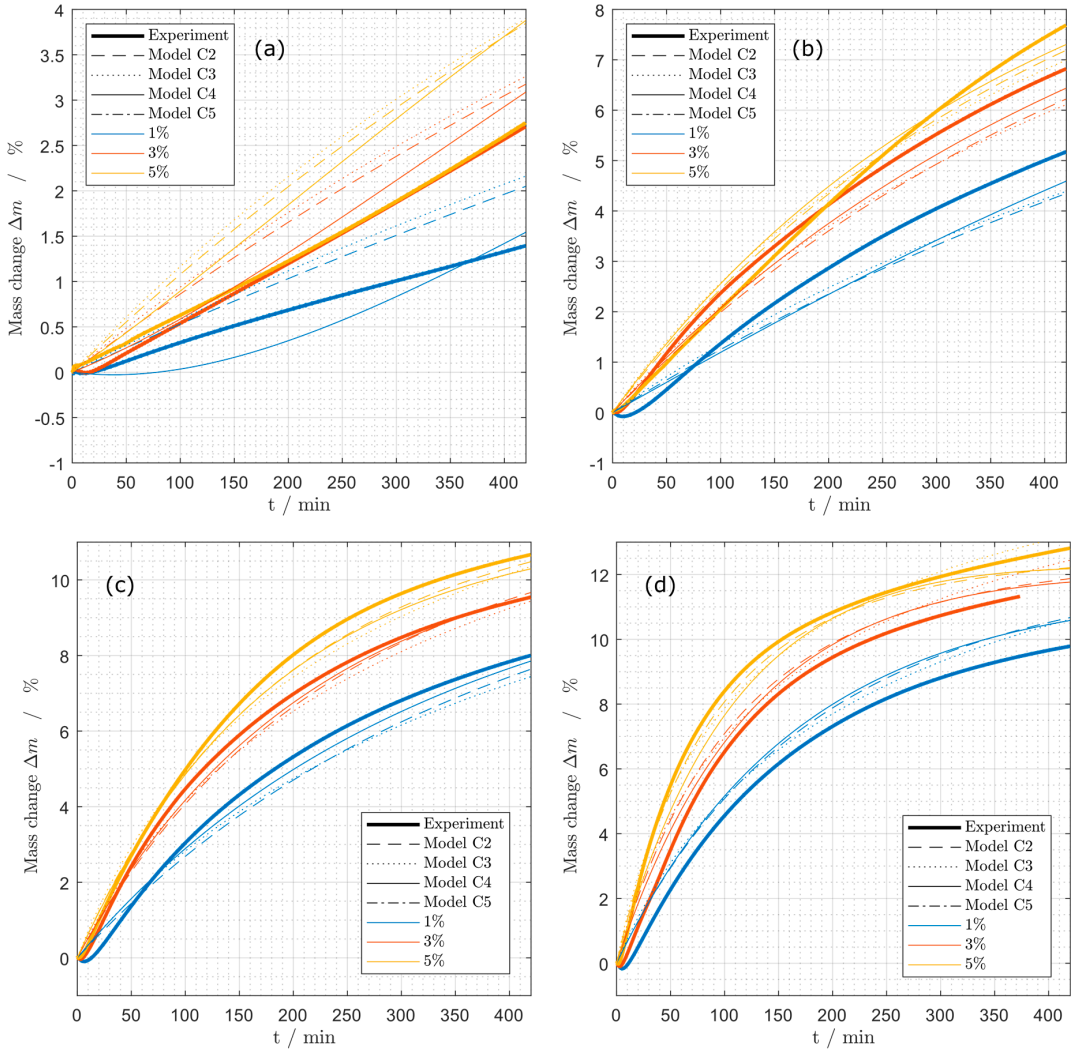

Figure 10. Mass change during coking experiments at different propane concentrations (1%, 3%, 5%) at (**a**) 575 °C, (**b**) 600 °C, (**c**) 625 °C and (**d**) 650 °C for the models (C2), (C3), (C4) and (C5) as used for coking from propene.

Table 7. Information criteria and comparison of the models (C2), (C3), (C4) and (C5) for deactivation using propane.

-	C2	C3	C4	C5
RSS_{opt}	4783.5	5509.6	3631.6	3631.6
p	7	5	9	7
AIC	28,225	31,070	22,675	22,671
$w(AIC)$	0.00%	0.00%	11.92%	88.08%

Table 8 shows the optimal parameters of the model and the corresponding confidence intervals, estimated by a bootstrapping procedure (Supplementary Material, parts B–C).

Table 8. Optimized parameters of model C5 to describe the coking behavior of the VO_x catalyst using propene.

Parameter	Opt. Value	Confidence Intervals		Unit
c_{max}	17.695	−1.54%	+1.35%	$\% \left(\frac{kg_{coke}}{kg_{cat}} \times 100\right)$
l	0.275	−2.05%	+1.55%	-
k_0	9.59×10^5	−29.71%	+33.72%	$\left(kg_{coke} kg_{cat}^{-1} \, min^{-1}\right)^{1-h}$
E_A	139,022	−1.92%	+1.35%	$J \, mol^{-1}$
h	1.106	−2.79%	+1.47%	-
k_{des}	3.22×10^{-3}	−2.24%	+4.09%	min^{-1}
c_0	5.994	−4.47%	+5.17%	$\% \left(\frac{kg_{coke}}{kg_{cat}} \times 100\right)$

Model (C5) does also not include a multilayer term. The difference between model (C3), which was chosen for the deactivations using propene and model (C5) is the missing desorption term in model (C3). The desorption does not play a significant role in describing the deactivation using propene due to the fast coking which dominates in the experiments. It has to be noted that these results are valid for the deactivation times realized in this study. Especially for propane a linear mass change at the end of the measurements for high temperatures can be observed, which leads to the conclusion that a linear multilayer term is suitable to describe the coking behavior for longer deactivation times [28,35]. This is an indicator that the systematic model reduction disregards a multilayer term that would be reasonable from a mechanistic point of view. A different experimental basis may lead to another model describing the coking of the catalyst.

In this section, a simple mathematical model was developed and validated to describe the coking behavior of the VO_x catalyst under a wide range of deactivation conditions. The models describe the mass change of the catalyst in good agreement with experimental data in a temperature range relevant for industrial processes. Keeping the total industrial production cycle in mind (see Figure 1), still a description of the regeneration of the catalyst is necessary. A mathematical model for the regeneration of the catalyst with oxygen is developed in the next section.

2.3. Catalyst Regeneration

For subsequent regeneration of the deactivated catalyst burn off of the coke is used. Different gases can be used for catalyst regeneration. The reactivity of these gases and therefore the gasification rates vary by orders of magnitudes [26]. Many processes, as introduced in Figure 1, use oxygen for regeneration of coked catalysts which has the advantage of the availability in air and reasonable gasification rates at moderate temperatures. In this contribution oxygen diluted in nitrogen was used for gasification.

To study the regeneration step, at first the catalyst was deactivated in long-term experiments using the described fixed bed reactor also used for the kinetic experiments (ID = 6mm, see Materials and Methods Section 3.2). To follow spatial developments, the catalyst bed was divided into three segments (Figure 11). Samples that were used for the regeneration experiments were deactivated at two different conditions (see Materials and Methods Section 3.4). The same TGA setup that was used for the deactivation experiments was also used for further regeneration experiments (Netzsch STA 445 F5 Jupiter). Samples deactivated under defined conditions and from different segments 1–3 of the catalyst bed were analyzed. The regeneration time was adjusted to the regeneration conditions. Low regeneration temperatures and low oxygen concentrations demand longer regeneration times because of their effect on the kinetics of the regeneration that will be discussed in this section.

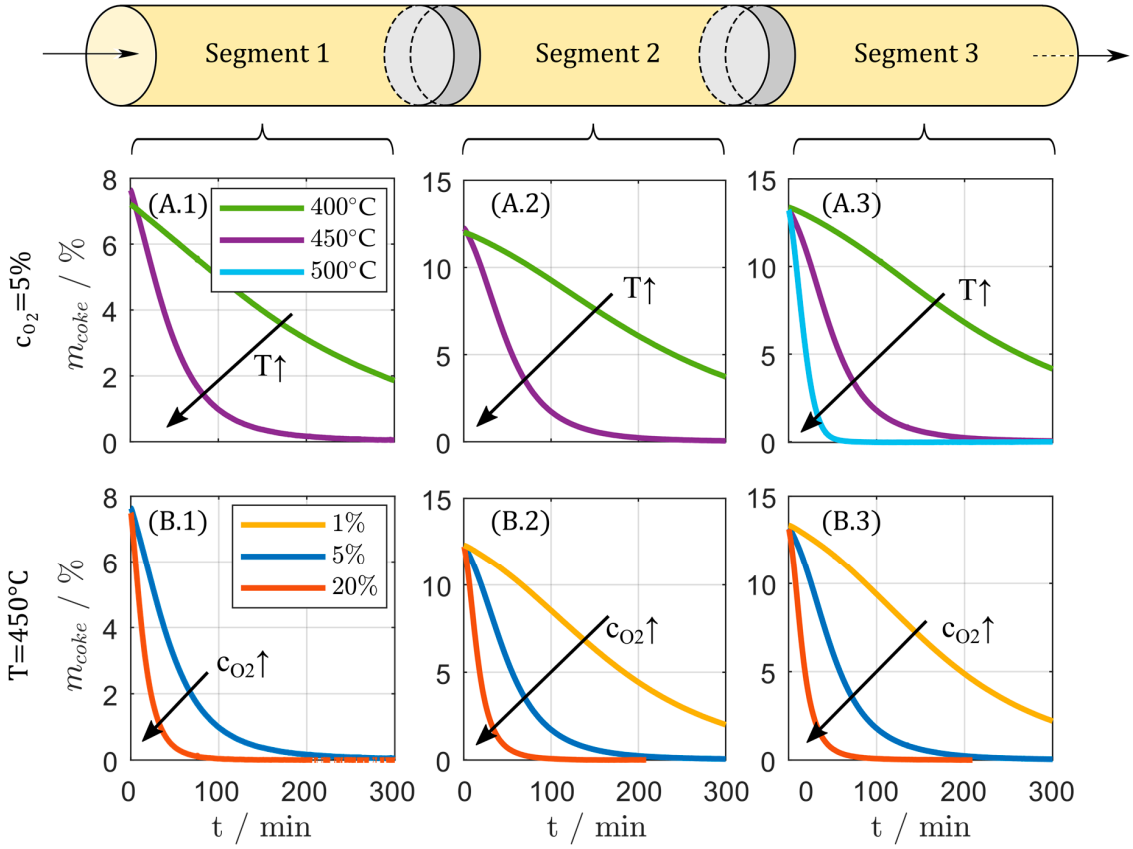

Figure 11. Regeneration behavior for samples from different catalyst segments in the lab scale fixed bed reactor at (**A**) constant oxygen concentration and (**B**) constant temperature and varied oxygen concentration for catalyst deactivated at deactivation condition 1.

Figures 11 and 12 show the mass changes during the regeneration experiments. It becomes obvious that a higher temperature leads to a faster regeneration (Figure 11(A.1–A.3) and Figure 12(A.1–A.3)). With increasing oxygen concentrations, the coke burning rate also increases significantly (Figure 11(B.1–B.3) and Figure 12(B.1–B.3)). The comparison the different segments of the catalyst bed reveals that more coke is deposited at the end of the catalyst bed in segment 3 (Figure 11). That supports the assumption that propene is the precursor for coking, since the propene concentration increases along the reactor length. At deactivation condition 1 (Table 12, Materials and Methods) the coke loading in the first catalyst segment 1 was only 7.4% (Figure 12(A.1,B.1)) whereas the coke loading at the last segment 3 was 13.3% (Figure 12(A.3,B.3)). A significant difference between the coke loading of the catalyst deactivated at the different conditions is also observable. With 13.3% the catalyst deactivated at condition 1 (Table 12) shows much more coking than the catalyst deactivated at condition 2 (1.7%). This is the effect of the elevated temperature of 600 °C at coking condition 1.

For the kinetic analysis it was assumed that the TGA is perfectly mixed and the oxygen is in high excess. For that reason, it can be assumed that the oxygen concentration is constant in the apparatus. The temperature dependency of the reaction rate constant was expressed with the Arrhenius equation (Equation (12)). Power law approaches to model coke burning kinetics based on TGA measurements are widely used in industry and research [36–38]. The results of these analyses can be used to design regenerators or regeneration strategies for fixed bed reactors [39,40]. A problem in estimating regeneration kinetics is the fact that coke depositions change their structure and their composition over time, a phenomenon known as coke aging. This can lead to difficulties in describing reliably coke burning kinetics. Differences in the behavior of the coke during regeneration can occur after different pretreatments but can also be observed in different parts of the reactor [38,41]. The aim of

this section is to develop a simplified kinetic model of the complex coke burning kinetics and to check whether these difficulties occur in the considered reaction system. To describe the complex kinetics of the regeneration the following power law approach was applied:

$$r = \frac{dm_{coke}}{dt} = k_{reg} \cdot m_{coke}^{\alpha} \cdot x_{O_2}^{\beta} \quad (29)$$

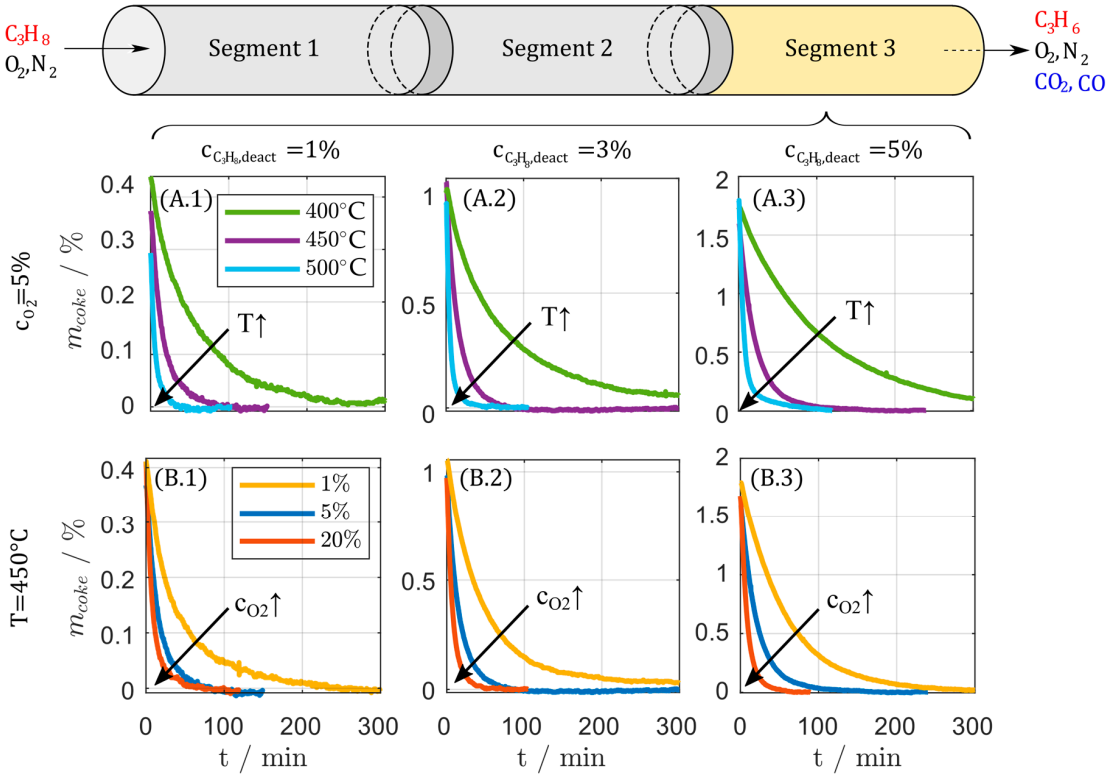

Figure 12. Regeneration behavior for samples from catalyst bed segment 3 in the lab scale fixed bed reactor at (**A**) constant oxygen concentration and (**B**) constant temperature and varied oxygen concentration for catalyst deactivated at deactivation condition 2.

The coke content m_{coke} is given in % (mass of coke per mass of fresh catalyst), in analogy to the deactivation experiments to make it possible to combine deactivation and regeneration models. x_{O_2} denotes the volume fraction of oxygen. It was crucial to make sure that samples selected from different segments of the reactor bed as well as samples of different coking experiments are part of the data set of this analysis. An overview of all experiments in the data set is given in the Materials and Methods section (Table 13).

The optimized parameters of the power law kinetics (Equation (29)) are listed in Table 9. The activation energy of 120 kJ mol^{-1} and the preexponential factor of 1.62×10^8 % min^{-1} are in the range of activation energies reported for dehydrogenation catalysts [42]. This is especially notable because the model in this contribution is not strictly mechanistic and can be seen as a simplification that lumps together the regeneration kinetics of different coke species that are supposed to be deposited at the different parts of the catalyst (support, active sites, etc.) Figure 13 illustrates experimental and simulated values of mass loss during the regeneration for catalyst deactivated at both deactivation conditions and regenerated at different conditions. The simulated mass loss during the regeneration is in good agreement with the experimental data for all experimental conditions covered. The simulated values reach a fully regenerated state earlier than the experimental values. Both deactivation conditions are fitted with a good precision. Figure 14a compares the regeneration for different segments of the

catalyst. The model is able to predict the mass loss for all segments with the same quality. Figure 14b shows a comparison between samples deactivated with different propane concentrations. Obviously, the different deactivation conditions have no influence on the goodness of the fit. Consequently, it can be stated that the model is able to describe the regeneration behavior for samples deactivated at different temperatures, over different times and at different propane concentrations with a good agreement and can be used for further model-based investigations and process optimization.

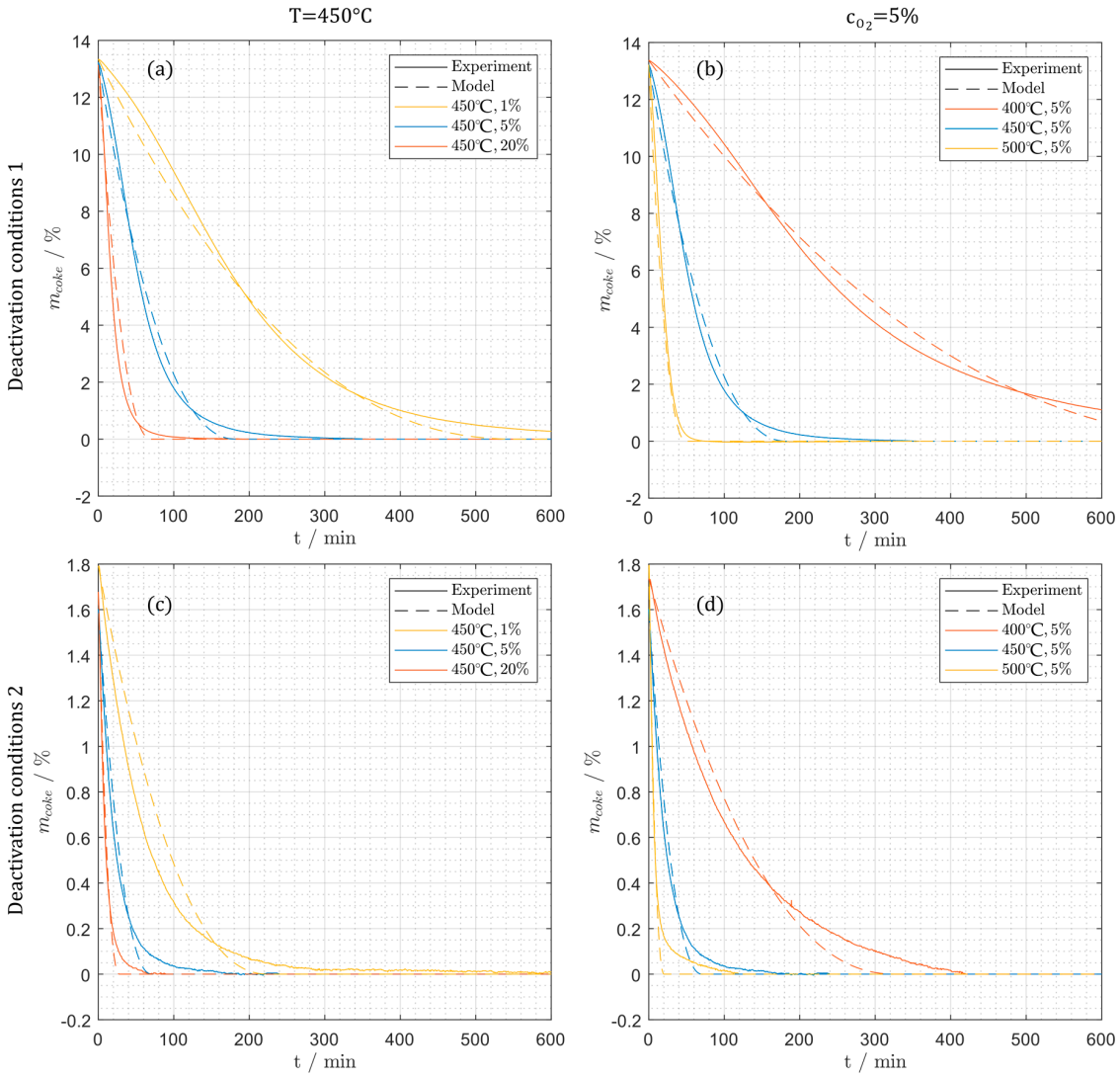

Figure 13. Comparison between the simulation and the experimental mass changes during regeneration for (**a**) deactivation condition 1 at varying oxygen concentration (1%, 5%, 20%), (**b**) deactivation condition 1 at different temperatures (400 °C, 450 °C, 500 °C), (**c**) deactivation condition 2 at different oxygen concentrations, (**d**) deactivation condition 2 at different temperatures.

Table 9. Optimal parameter for the regeneration model (Equation (29)).

Parameter	Opt. Value		Unit
$k_{0,reg}$	1.62×10^8	± 2.63%	% min^{-1}
$E_{A,reg}$	120,835.9	± 0.12%	J mol^{-1}
α	0.5517	± 0.12%	-
β	0.6859	± 0.16%	-

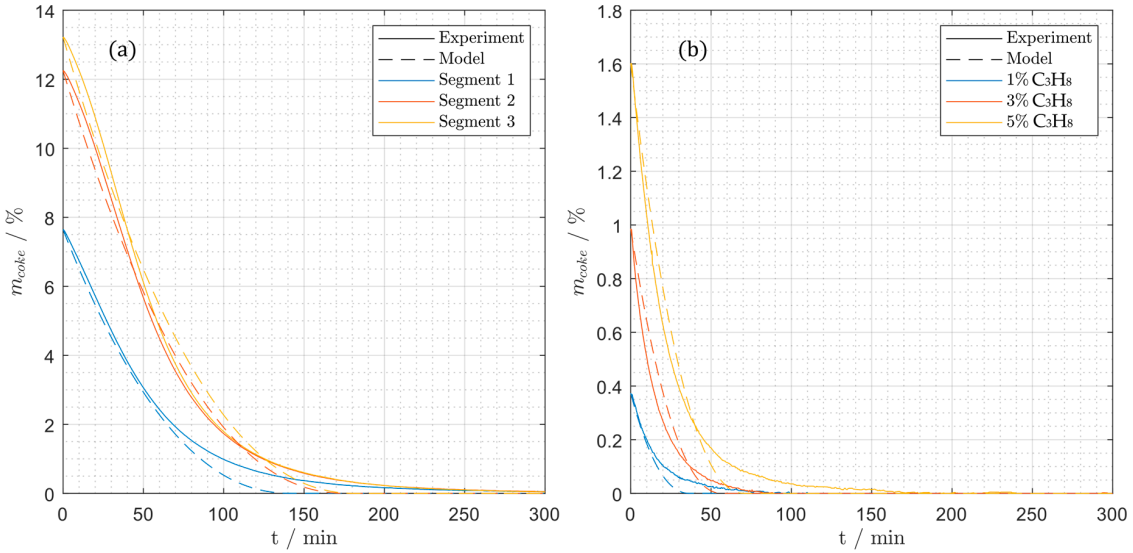

Figure 14. (**a**) Comparison of the regeneration of different segments of the catalyst packing deactivated at deactivation condition 1, (**b**) influence of propane concentration (1%, 5%, 20%) on coke loading in segment 3 (deact. condition 2).

2.4. Periodic Experiments and Validation

For validation of the parameterized kinetic models for catalyst deactivation and reactivation, different, sequential periodic experiments using the TGA setup were conducted. All periodic experiments consist of three deactivation phases followed by regeneration phases. The periodic operation was used to verify the validity of the mathematical models including the derived parameters and to check the stability of the catalyst and reproducibility under periodic operation. Propane was used during the deactivation phase as a simplified industrial feed [7].

Three different periodic experiments were conducted for this study (see Materials and Methods). Either the deactivation phase or the regeneration phase was varied between the experiments. The deactivation phases were performed at 625 °C for 120 min. Regeneration phases were performed at lower temperatures of 450 °C and 500 °C to avoid structural changes of the catalyst by local hotspots. This was considered to make sure that similar experiments can be performed in pilot and industrial scale equipment where local hotspots play an important role. The regeneration time in all experiments was 60 min.

Mass changes of the sample and measured temperature during the periodic experiments (1) (see Table 15) are shown in Figure 15a. At the beginning of the experiment, the sample was heated up to reaction temperature. During this initial heat up phase a significant mass loss due to desorption can be observed. After the equilibration phase, propane was introduced to the system and there is another small mass loss observable at the beginning of the deactivation phase. This result is in accordance to the observations of the deactivation experiments described before. After that the mass of the sample increased due to coke built up until the deactivation phase was ended. Figure 15c illustrates the change in the product gas composition during the deactivation phase. Since the TGA setup is not able to continue the measurement with another gas, the operator had to change settings at the experimental setup manually which causes disturbances in the TGA signal as well as in the temperature signal directly after the deactivation phase. A drop in temperature was unavoidable so that the setup had to be heated up to the regeneration temperature after changing the settings. In Figure 15b the measured oxygen concentration at the outlet of the experimental setup and the inlet concentrations are shown. At the beginning of the regeneration phase, the concentrations of the inlet flow differs from the concentration of the outlet flow due to the consumption of oxygen during the regeneration. Simultaneously, a spike in the concentrations of the product gases of the regeneration

(CO, CO_2, Figure 15c) was detected. The concentration of CO_2 is at every point significantly higher than the concentration of CO, which indicates that enough oxygen for a total oxidation of coke is provided. Over the course of the regeneration phase the oxygen concentration at the outlet converged to the inlet concentration. The decreasing product gas concentrations indicated that the gasification reactions are completed at the end of the regeneration phase, as can be seen in the mass signal, too. Similar figures for the periodic experiments (2) and (3) can be found in the Supplementary Material, part D. A trend that is observable in all periodic experiments is a shift of the sample mass. It has to be checked in further experiments if this shift diminishes over the course of more cycles.

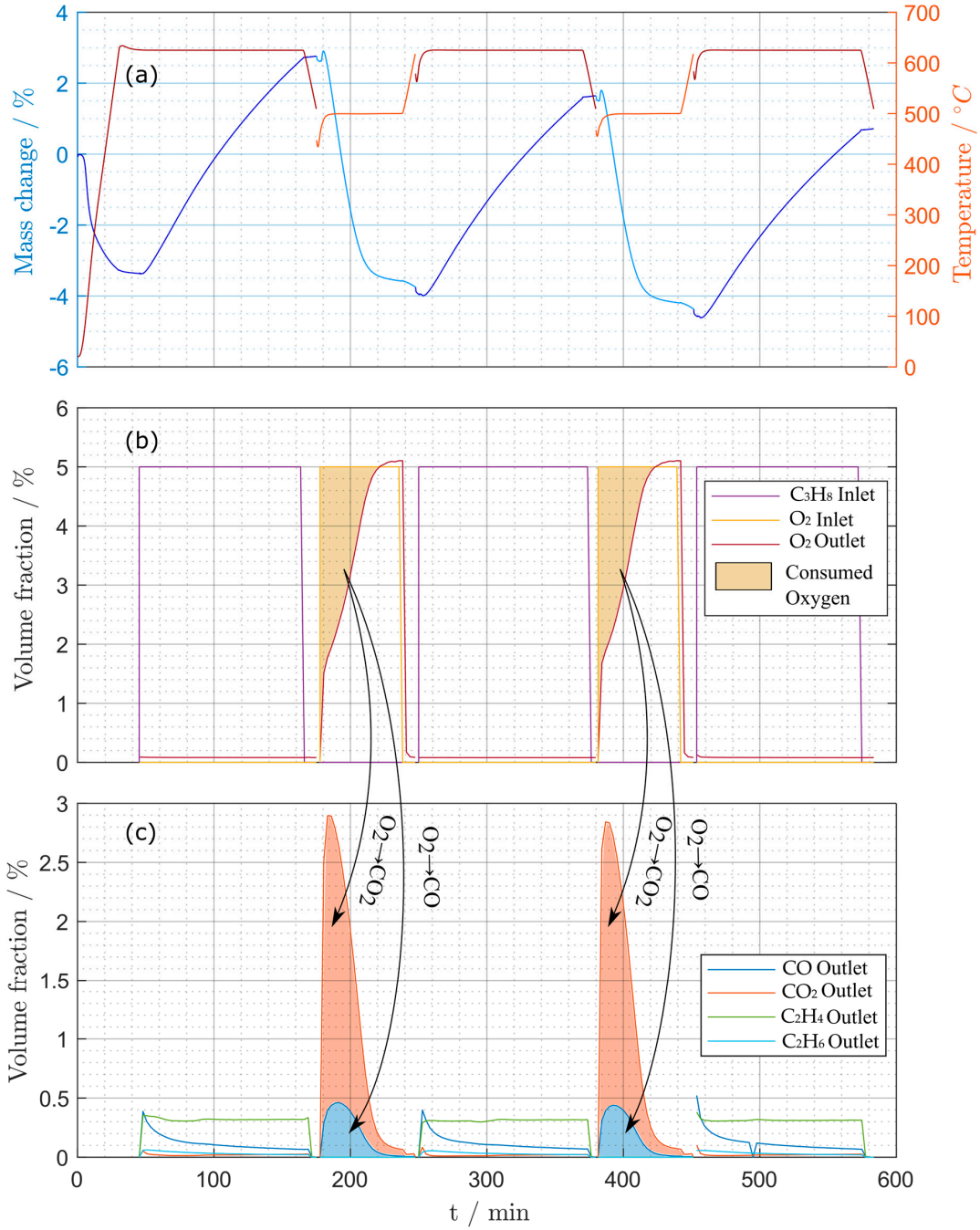

Figure 15. Measurements during periodic experiments: (**a**) mass changes (TGA) and temperature, (**b**) oxygen and propane concentrations, (**c**) CO, CO_2, ethene and ethane concentrations for periodic experiment (1).

Considering all results, the periodic experiments indicate a good long-term stability of the catalyst. Deactivation as well as regeneration phases are reproducible. The reproducibility of the regeneration phase is also shown in Figure 16 where the product gas concentration and the oxygen concentrations of the different regeneration phases are depicted.

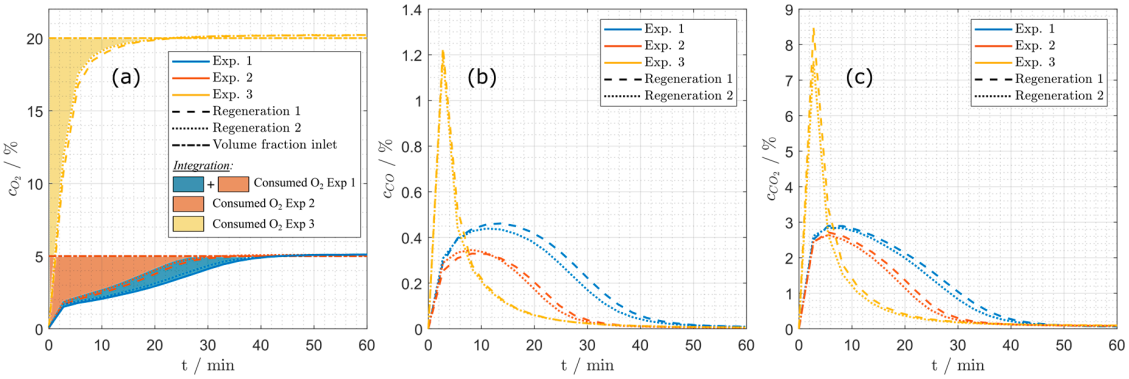

Figure 16. Comparison of measured concentrations during all regeneration phases: (**a**) oxygen, (**b**) CO, (**c**) CO_2 (for experimental conditions see Table 15).

The concentration curves of CO and CO_2 were also used to calculate the amount of carbon that was gasified. These calculations are compared to the mass loss recorded by the TGA in Table 10. The calculated carbon mass is generally in accordance with the TGA measurements but overestimates the mass loss. The source of this difference is unclear. Coking of the inner parts of the TGA oven cannot be excluded.

Table 10. Comparison between gasified carbon and mass loss recorded by the TGA (for experimental conditions see Table 15).

-	-	Exp 1		Exp 2		Exp 3	
-	-	**Reg 1**	**Reg 2**	**Reg 1**	**Reg 2**	**Reg 1**	**Reg 2**
GC	Mass carbon (combustion products)/mg	43.41	40.49	30.25	28.19	30.16	26.43
TGA	Total mass change/mg	42.07	39.29	27.27	25.55	28.44	25.11
-	Deviation carbon content: GC vs. TGA	3.18%	3.06%	10.93%	10.33%	6.05%	5.24%

Finally, to verify the models of deactivation and regeneration a simulation of the periodic experiments was conducted. Model C5 (Equation (28)) was used to simulate the deactivation phase and the power law approach (Equation (29)) was used to simulate the regeneration phase with the parameters given in Tables 8 and 9. The results are shown in Figure 17.

Due to the manual changes between the regeneration and deactivation phase an ideal behavior cannot be observed in the periodic experiments performed. For that reason, calculated mass changes were normalized to the actual mass at the beginning of the respective phase in Figure 17 and a very good agreement of the experimental and the simulated data can be recognized.

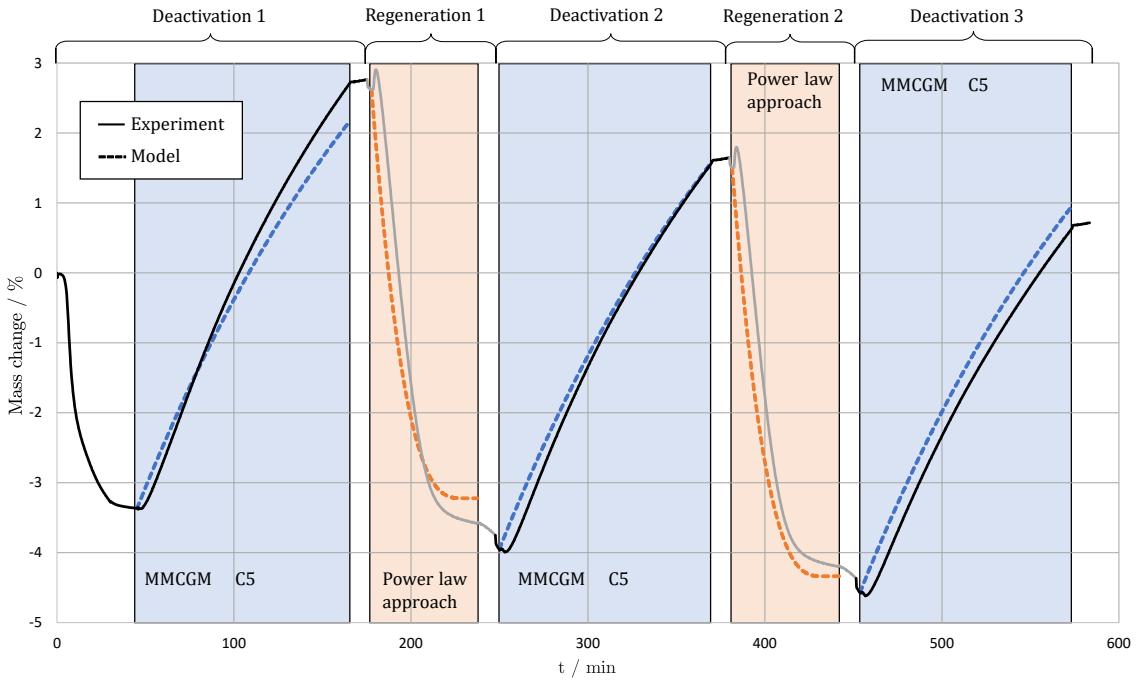

Figure 17. Experimental (TGA) and simulated mass changes during periodic experiment 1 (for experimental conditions see Table 15).

3. Materials and Methods

3.1. Catalyst Preparation

The catalyst was prepared via impregnation of γ-Al_2O_3 spheres (diameter: 1 mm, specific area: 168 m^2 g^{-1}) with vanadyl acetylacetonate in acetone. The impregnated catalyst was washed, dried and calcinated. The vanadium content of the catalyst was 1.4% and its specific surface area amounts 158 m^2 g^{-1} (BET) [15–18].

3.2. Kinetic Investigation of the Reaction Network

3.2.1. Laboratory-Scale Fixed Bed Reactor Setup

For the parametrization of the kinetic model, lab scale experiments in a quartz glass fixed bed reactor were conducted. The inner diameter (ID) of the reactor was 6 mm. The temperature range was varied between 350 °C and 600 °C. Weight hourly space velocities (WHSV) of 100, 200 and 400 kg s m^{-3} were applied. The mass of the catalyst used for these experiments was either 1.5 g or 0.75 g which results in a bed length of around 6 cm/3 cm. A variation of the catalyst mass was necessary due to the limitations of the experimental setup, mainly the ranges of the mass flow controllers (MFCs). The quartz glass tube was heated by an electric oven and the temperature in the middle of the catalyst bed was measured with a thermocouple. The temperature of the oven was controlled according to the temperature in the middle of the catalyst bed to assure isothermal conditions during the measurements. For safety reasons, the propane and the oxygen concentration were varied between 0% and the lower explosion limit of around 1% [43]. Experiments without oxygen were performed up to a maximum propane concentration of 5%. All gas flows were controlled by MFCs. The composition of the gas flows at the reactor inlet and at the reactor outlet were analyzed by GC measurements (Agilent Technologies 7890B GC System).

3.2.2. Modeling of the Reaction Network

To estimate the kinetic parameters a 1D plug flow model of the reactor was implemented in MATLAB®. Steady state as well as isobar and isothermal conditions were assumed. Equation (30)

shows the mass balance of component i using the molar flux $\dot{n}_i$. M describes the total amount of reactions, m_{cat} the mass of the catalyst and z the axial length, where Z represents the length of the reactor.

$$\frac{d\dot{n}_i}{dz} = \frac{m_{cat}}{Z} \cdot \sum_{j=1}^{M} \nu_{i,j} \cdot r_{j,m} \tag{30}$$

The lsqnonlin function of MATLAB® was used for optimizing the kinetic parameters Γ_{kin} by minimizing the objective function (Equation (31)), where N_{exp} is the absolute number of all conducted experiments ($N_{exp} = 269$) and K are the experimentally (exp) or simulative (sim) investigated propane conversion $X_{C_3H_8}$ (Equation (32)), propene selectivity $S_{C_3H_6}$, CO_2 selectivity S_{CO_2} and CO selectivity S_{CO} (Equation (33)). Γ_{kin} denotes the set kinetic parameters of the reaction network.

$$\textit{Objective Function}: \quad OF_{kin} = \min_{\Gamma} RSS = \sum_{l=1}^{N_{exp,kin}} \left[K_l^{exp} - K_l^{sim}(\Gamma_{kin}) \right]^2 \tag{31}$$

$$\textit{Conversion}: \quad X_{C_3H_8} = \frac{\dot{n}_{C_3H_8}^{in} - \dot{n}_{C_3H_8}(z = Z)}{\dot{n}_{C_3H_8}^{in}} \tag{32}$$

$$\textit{Selectivity}: \quad S_i = \frac{\dot{n}_i(z = Z) - \dot{n}_i^{in}}{\dot{n}_{C_3H_8}^{in} - \dot{n}_{C_3H_8}(z = Z)}, \qquad i \in \{C_3H_6,\ CO_2,\ CO\} \tag{33}$$

3.3. Catalyst Deactivation

3.3.1. Experimental Setup and Procedure

To investigate the coking behavior of the catalyst experimentally, a TGA setup with three MFCs was used (Netzsch STA 445 F5 Jupiter). The WHSV during the experiments was set to 400 kg s m^{-3} and the overall gas flow was set to 100 mL min^{-1}. The resulting mass of the catalyst sample was 666 mg. Propene and propane were used as precursors for coking. The concentration of hydrocarbons was varied between 1%, 3% and 5%. A coking experiment started with evacuating the setup twice and flushing it with nitrogen to assure an inert atmosphere. The sample was then heated up to reaction temperature and after an equilibration time of 15 min the hydrocarbon was introduced to the system. The deactivation time was 7 h. An overview of all experiments used for parameter estimation is illustrated in Table 11.

Table 11. Data set for kinetic analysis of the deactivation kinetics of the catalyst (PA: propane; PE propene; ✓: tested; ✗: not tested).

-	575 °C	600 °C	625 °C	650 °C
-	**PA/PE**	**PA/PE**	**PA/PE**	**PA/PE**
1%	✓/✓	✓/✓	✓/✓	✓/✓
3%	✓/✓	✓/✓	✓/✓	✗/✓
5%	✓/✓	✓/✓	✓/✓	✓/✓

Over the whole course of the experiment the concentration of the gases at the outlet of the TGA setup were monitored by online GC measurements (Agilent 490 Micro GC, Channel 1: 10 m Molsieve 5 Å, Channel 2: 10 m PPU; Detectors: TCD).

3.3.2. Analysis of Deactivation Experiments

The kinetic parameters of the deactivation models Γ_{deact} were used to fit the experimental data. For estimating the parameters based on the experimental results the lsqnonlin solver of MATLAB® was used to minimize the objective function (Equation (34)).

$$OF_{deact} = \min_{\Gamma} RSS = \sum_{l=1}^{N_{exp,deact}} \left[c_{coke,l}^{exp} - c_{coke,l}^{sim}(\Gamma_{deact})\right]^2 \quad (34)$$

3.4. Catalyst Regeneration

3.4.1. Experimental Setup and Procedure

Samples for regeneration experiments were deactivated in long-term experiments using a quartz glass lab scale reactor also used for the kinetic experiments (ID = 6 mm). The catalyst bed was divided into three segments (Figure 11), 0.5 g catalyst each, separated by quartz glass wool. Samples that were used for the regeneration experiments were deactivated at two different conditions which are given in detail in Table 12.

Table 12. Deactivation conditions of the samples used in regeneration experiments.

-	Deactivation Condition 1	Deactivation Condition 2
Temperature	600 °C	500 °C
Propane concentration	5%	1%, 3%, 5%
Oxygen concentration	0%	0%
Deactivation time	48 h	96 h
WHSV	400 kg s m^{-3}	400 kg s m^{-3}
Tested segment	1, 2, 3	3

The first deactivation condition consists of a 48 h deactivation period at 600 °C, 5% propane and a WHSV of 400 kg s m^{-3}. At deactivation condition 1 samples of all three segments of the catalyst bed were used for regeneration experiments in the TGA (Figure 11).

The second deactivation condition includes a 96 h time period at 500 °C. The propane concentration was varied between 1%, 3% and 5%. Since the built up of coke on the catalyst is less severe at deactivation condition 2, only the third segment of the catalyst bed was analyzed, due to the higher coke concentration in this part of the reactor compared to the other segment closer to the reactor inlet (Figure 13).

The same TGA setup described above that was used for the deactivation experiments was also applied for the regeneration experiments (Netzsch STA 445 F5 Jupiter). The standard sample size in regeneration experiments was 80 mg. Before starting a regeneration measurement, the TGA setup was evacuated and flushed with nitrogen twice to ensure an inert environment. After heating up the TGA to a starting temperature of 100 °C the sample was heated up to the desired regeneration temperature with 20 K min^{-1}. After an equilibration period of 15 min the oxygen was introduced to the system and the mass change was recorded by the TGA until the end of the regeneration time. The whole experiment was monitored simultaneously by Micro GC measurements.

Table 13 summarizes all experiments that were used for the parameter estimation of the regeneration model (Equation (29)).

Table 13. Deactivation conditions of the samples used in regeneration experiments.

-	-	Activation Condition				
-	-	450 °C, 5% Oxygen	450 °C, 20% Oxygen	400 °C, 5% Oxygen	450 °C, 1% Oxygen	500 °C, 5% Oxygen
Deactivation condition 1	Segment 1	✓	✓	✓	✗	✗
	Segment 2	✓	✓	✓	✓	✗
	Segment 3	✓	✓	✓	✓	✓
Deactivation condition 2	1% propane	✓	✓	✓	✓	✓
	3% propane	✓	✓	✓	✓	✓
	5% propane	✓	✓	✓	✓	✓

An overview of the different regeneration times is given in Table 14.

Table 14. Regeneration times for different regeneration conditions.

-	1% O_2	5% O_2	20% O_2
400 °C	-	24.5 h	-
450 °C	18.5 h	6.5 h	3 h
500 °C	-	2.5 h	-

3.4.2. Analysis of Deactivation Experiments

In analogy to the kinetic analyses of the main reaction network and the deactivation kinetics the parameters Γ_{reg} for the regeneration kinetics were estimated by using the lsqnonlin routine in MATLAB® with a corresponding objective function (Equation (35))

$$OF_{reg} = \min_{\Gamma} RSS = \sum_{l=1}^{N_{exp,reg}} \left[c_{coke,l}^{exp} - c_{coke,l}^{sim}\left(\Gamma_{reg}\right)\right]^2 \quad (35)$$

3.5. Periodic Experiments and Validation

Experimental Setup and Procedure

For periodic experiments the TGA setup was used, coupled with an online Micro GC as described above. The concentration of oxygen was varied between 5% and 20%. For an overview of the experimental conditions of all three periodic experiments see Table 15.

Table 15. Experimental conditions of the deactivation and regeneration phase of the periodic experiments.

-	Deactivation				Regeneration			
Exp	**T/°C**	**t/min**	$\dot{V}_{C_3H_8}$/mL/min	$c_{C_3H_8}$/%	**T/°C**	**t/min**	$\dot{V}_{O_2}$/mL/min	c_{O_2}/%
(1)	625	120	5	5	500	60	24	5
(2)	625	120	1	1	500	60	24	5
(3)	625	120	1	1	450	60	95	20

Between the individual sequences during the periodic operation it is necessary to cool down the instrument from the deactivation temperature to the regeneration temperature and vice versa. The time required was also used to purge the unit from the reaction gases to avoid the formation of explosive gas mixtures.

The deactivation sequences started with evacuating and flushing the TGA twice with nitrogen. The sample was then heated up to the deactivation temperature with a heating rate of 20 K min^{-1}. After 15 min of equilibration the coking was started by introducing the intended amount of propane to the gas flow. After 120 min the gas composition was changed to nitrogen only and the instrument cooled down to 500 °C or 450 °C with a cooling rate of 12.5 K min^{-1}. The cooling procedure takes 10 min or 14 min, respectively. In preliminary experiments it was checked that a 10 min time span for cooling is also sufficient to flush out propane to be able to safely introduce oxygen without operating within the explosion limits.

The regeneration sequence started by introducing the selected oxygen concentration to the system at a temperature of 500 °C or 450 °C, respectively. After 60min the gas composition was changed to nitrogen and the setup was heated up to 625 °C with 12.5 K min^{-1} to reach deactivation temperature and to reject all oxygen from the system. Throughout the experiments, the composition of the gases at the outlet of the TGA were monitored using Micro GC. Mass and temperatures changes were recorded by the TGA system itself. For an overview of the periodic experiments see Figure 15 and Figures S2 and S3.

4. Conclusions and Outlook

The aim of this contribution was the experimental and model-based investigation of the deactivation and regeneration of a VO_x catalyst during the thermal and oxidative dehydrogenation of propane in order to understand and optimize established processes and to develop new reactor concepts, respectively.

The kinetic models developed in this contribution are all able to describe the complex behavior of the VO_x catalyst with good agreement. An empirical power law model was able to describe the kinetic network and kinetics of propane dehydrogenation (ODH + TDH) in a wide range of experimental conditions. Propene was identified as the main precursor for coke formation. Coking kinetics were quantified to be able to describe the coke growth during long-term production cycles caused by TDH. This kinetics were modeled using multilayer-monolayer coke growth models of different complexity. Approaches from literature were extended by to describe the influence of the precursor concentrations. A systematic model discrimination was applied to find a suitable model. Gasification of the coke deposits was described by a power law approach. It was shown that the corresponding model is able to describe the regeneration behavior regardless of the position of the coke in the reactor and the coking conditions.

On the basis of the derived and parametrized models it is possible to carry out detailed transient simulations of conventional fixed bed reactors with locally different coke built up related to the local propene concentrations. The subsequent regeneration of the coke distributed across the reactor length can also be simulated. The results show that also the consumption of oxygen is this process can be described.

Ongoing studies will provide simulations of more complex, periodically operated reactor setups (Figure 18) and the evaluation regarding their performance in comparison to conventional reactors [15]. Innovative setups allow combining TDH and ODH in one integrated reactor that consists of two concentric tubes. The outer tube is realized as a membrane to allow a distributed reactant dosing. Flow reversal enables switching between regeneration and ODH phase and TDH phase in the same apparatus. One missing link and subject of further studies is the exploration of the connection between coking and activity loss (Figure 2) [44,45].

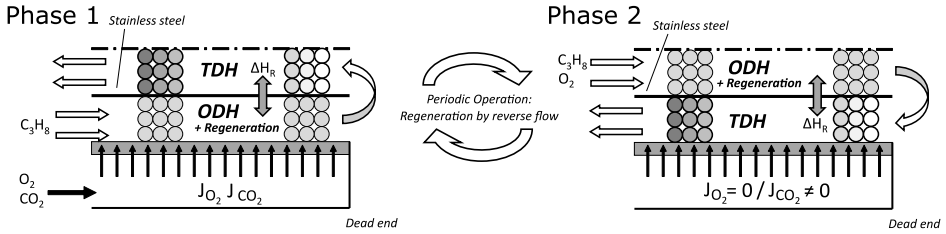

Figure 18. Integrated membrane reactor concept for periodic operation of the reactor including operando regeneration by flow reversal.

In summary, a comprehensive mathematical model covering all aspects of relevance regarding the catalyst performance was established in this contribution. This model allows a detailed non-steady state reactor simulation as basis for optimization of established reactors and for designing new reactor concepts (Figure 18).

Supplementary Materials: The following are available online at http://www.mdpi.com/2073-4344/10/12/1374/s1, Table S1: Optimized kinetic parameters for the reaction network of the dehydrogenation of propane, Table S2: Preexponential factors and activation energies for the reaction network of the dehydrogenation of propane derived from the optimized parameters (Table S1), Table S3: Optimized parameters of model C5 to describe the coking behavior of the VO_x catalyst using propene, Figure S1: Histograms of the distribution of the parameters of the bootstrapping process of model (C5) of the deactivation of the VO_x catalyst with propene, Figure S2. Measurements during periodic experiments: (a) mass changes (TGA) and temperature, (b) oxygen concentration and propane concentration, (c) CO, CO_2, ethene and ethane concentration for periodic experiment (2), Figure S3. Measurements during periodic experiments: (a) mass changes (TGA) and temperature, (b) oxygen concentration and propane concentration, (c) CO, CO_2, ethene and ethane concentration for periodic experiment (3).

Author Contributions: Conceptualization, C.H.; Methodology, A.B. and C.H.; Software, A.B.; Validation, A.B.; Formal Analysis, A.B.; Investigation, A.B.; Resources, C.H.; Writing—Original Draft Preparation, A.B.; Writing—Review & Editing, C.H. and A.S.-M.; Visualization, A.B.; Supervision, C.H.; Project Administration, C.H. and A.S.-M.; Funding Acquisition, C.H. and A.S.-M. All authors have read and agreed to the published version of the manuscript.

Funding: The financial support of the German Science Foundation (projects: "Kontrolle und Intensivierung von Reaktionen durch Einsatz zyklisch betriebener Distributoren" (SE 568/23-1/HA 6762/2-1) and SFB/TRR 63: "InPROMPT—Integrated Chemical Processes in Multi-Phase Fluid Systems") is gratefully acknowledged.

Acknowledgments: The authors thank Jutta Wilke for the technical assistance at the FBR experiments and Anne Baier and Renate Zinke for the technical assistance at the TGA experiments.

Conflicts of Interest: The authors declare no conflict of interest.

References

1. Amghizar, I.; Vandewalle, L.A.; van Geem, K.M.; Marin, G.B. New Trends in Olefin Production. *Engineering* **2017**, *3*, 171–178. [CrossRef]
2. Nakaya, Y.; Hirayama, J.; Yamazoe, S.; Shimizu, K.-I.; Furukawa, S. Single-atom Pt in intermetallics as an ultrastable and selective catalyst for propane dehydrogenation. *Nat. Commun.* **2020**, *11*, 2838. [CrossRef] [PubMed]
3. Kotanjac, Ž.S.; van Sint Annaland, M.; Kuipers, J.A.M. Demonstration of a packed bed membrane reactor for the oxidative dehydrogenation of propane. *Chem. Eng. Sci.* **2010**, *65*, 6029–6035. [CrossRef]
4. Matveyeva, A.N.; Wärnå, J.; Pakhomov, N.A.; Murzin, D.Y. Kinetic modeling of isobutane dehydrogenation over Ga_2O_3/Al_2O_3 catalyst. *Chem. Eng. J.* **2020**, *381*, 122741. [CrossRef]
5. Matveyeva, A.N.; Zaitseva, N.A.; Mäki-Arvela, P.; Aho, A.; Bachina, A.K.; Fedorov, S.P.; Murzin, D.Y.; Pakhomov, N.A. Fluidized-Bed Isobutane Dehydrogenation over Alumina-Supported Ga_2O_3 and Ga_2O_3–Cr_2O_3 Catalysts. *Ind. Eng. Chem. Res.* **2018**, *57*, 927–938. [CrossRef]
6. Eisele, P.; Killpack, R. Propene. In *Ullmann's Encyclopedia of Industrial Chemistry*; Wiley: Chichester, UK, 2010; p. 101. ISBN 3527306730.
7. Won, W.; Lee, K.S.; Lee, S.; Jung, C. Repetitive Control and Online Optimization of Catofin Propane Process. *IFAC Proc. Vol.* **2009**, *42*, 273–278. [CrossRef]

8. Farsi, M.; Jahanmiri, A.; Rahimpour, M.R. Steady state modeling and simulation of the Oleflex process for isobutane dehydrogenation considering reaction network. *Asia-Pac. J. Chem. Eng.* **2013**, *8*, 862–869. [CrossRef]
9. Keil, F.J. Process intensification. *Rev. Chem. Eng.* **2018**, *34*, 135–200. [CrossRef]
10. Gallucci, F.; Antonio Medrano, J.; Roses, L.; Brunetti, A.; Barbieri, G.; Viviente, J. Process Intensification via Membrane Reactors, the DEMCAMER Project. *Processes* **2016**, *4*, 16. [CrossRef]
11. Rieck Genannt Best, F.; Mundstock, A.; Dräger, G.; Rusch, P.; Bigall, N.C.; Richter, H.; Caro, J. Methanol-to-Olefins in a Membrane Reactor with in situ Steam Removal—The Decisive Role of Coking. *ChemCatChem* **2020**, *12*, 273–280. [CrossRef]
12. Caro, J. Basic Aspects of Membrane Reactors. In *Comprehensive Membrane Science and Engineering*; Drioli, E., Ed.; Elsevier: Amsterdam, The Netherlands, 2010; pp. 1–24. ISBN 9780080932507.
13. Cruellas, A.; Ververs, W.; van Annaland, M.S.; Gallucci, F. Experimental Investigation of the Oxidative Coupling of Methane in a Porous Membrane Reactor: Relevance of Back-Permeation. *Membranes* **2020**, *10*, 152. [CrossRef] [PubMed]
14. Cruellas, A.; Heezius, J.; Spallina, V.; van Sint Annaland, M.; Medrano, J.A.; Gallucci, F. Oxidative Coupling of Methane in Membrane Reactors; A Techno-Economic Assessment. *Processes* **2020**, *8*, 274. [CrossRef]
15. Brune, A.; Wolff, T.; Seidel-Morgenstern, A.; Hamel, C. Analysis of Membrane Reactors for Integrated Coupling of Oxidative and Thermal Dehydrogenation of Propane. *Chem. Ing. Tech.* **2019**, *56*, 251. [CrossRef]
16. Hamel, C.; Tóta, Á.; Klose, F.; Tsotsas, E.; Seidel-Morgenstern, A. Analysis of single and multi-stage membrane reactors for the oxidation of short-chain alkanes—Simulation study and pilot scale experiments. *Chem. Eng. Res. Des.* **2008**, *86*, 753–764. [CrossRef]
17. Hamel, C.; Wolff, T.; Subramaniam, P.; Seidel-Morgenstern, A. Multicomponent Dosing in Membrane Reactors Including Recycling—Concept and Demonstration for the Oxidative Dehydrogenation of Propane. *Ind. Eng. Chem. Res.* **2011**, *50*, 12895–12903. [CrossRef]
18. Klose, F. Selective oxidation of ethane over a VO_x/γ-Al_2O_3 catalyst—Investigation of the reaction network. *Appl. Catal. A* **2004**, *260*, 101–110. [CrossRef]
19. Sheintuch, M.; Nekhamkina, O. Architecture alternatives for propane dehydrogenation in a membrane reactor. *Chem. Eng. J.* **2018**, *347*, 900–912. [CrossRef]
20. Peters, T.A.; Liron, O.; Tschentscher, R.; Sheintuch, M.; Bredesen, R. Investigation of Pd-based membranes in propane dehydrogenation (PDH) processes. *Chem. Eng. J.* **2016**, *305*, 191–200. [CrossRef]
21. Schäfer, R.; Noack, M.; Kölsch, P.; Stöhr, M.; Caro, J. Comparison of different catalysts in the membrane-supported dehydrogenation of propane. *Catal. Today* **2003**, *82*, 15–23. [CrossRef]
22. Shelepova, E.V.; Vedyagin, A.A. Intensification of the dehydrogenation process of different hydrocarbons in a catalytic membrane reactor. *Chem. Eng. Process. Process. Intensif.* **2020**, *155*, 108072. [CrossRef]
23. Fouty, N.J.; Carrasco, J.C.; Lima, F.V. Modeling and Design Optimization of Multifunctional Membrane Reactors for Direct Methane Aromatization. *Membranes* **2017**, *7*, 48. [CrossRef] [PubMed]
24. Hou, K.; Hughes, R. The kinetics of methane steam reforming over a Ni/α-Al2O catalyst. *Chem. Eng. J.* **2001**, *82*, 311–328. [CrossRef]
25. Schwaab, M.; Pinto, J.C. Optimum reference temperature for reparameterization of the Arrhenius equation. Part 1: Problems involving one kinetic constant. *Chem. Eng. Sci.* **2007**, *62*, 2750–2764. [CrossRef]
26. Argyle, M.; Bartholomew, C. Heterogeneous Catalyst Deactivation and Regeneration: A Review. *Catalysts* **2015**, *5*, 145–269. [CrossRef]
27. Sokolov, S.; Bychkov, V.Y.; Stoyanova, M.; Rodemerck, U.; Bentrup, U.; Linke, D.; Tyulenin, Y.P.; Korchak, V.N.; Kondratenko, E.V. Effect of VO_x Species and Support on Coke Formation and Catalyst Stability in Nonoxidative Propane Dehydrogenation. *ChemCatChem* **2015**, *7*, 1691–1700. [CrossRef]
28. Gascón, J.; Téllez, C.; Herguido, J.; Menéndez, M. Propane dehydrogenation over a Cr2O3/Al2O3 catalyst: Transient kinetic modeling of propene and coke formation. *Appl. Catal. A* **2003**, *248*, 105–116. [CrossRef]
29. Spiess, A.-N.; Neumeyer, N. An evaluation of R^2 as an inadequate measure for nonlinear models in pharmacological and biochemical research: A Monte Carlo approach. *BMC Pharmacol.* **2010**, *10*, 6. [CrossRef]
30. Burnham, K.P.; Anderson, D.R. *Model Selection and Multimodel Inference*; Springer: New York, NY, USA, 2004.
31. Akaike, H. A Bayesian analysis of the minimum AIC procedure. *Ann. Inst. Stat. Math.* **1978**, *30*, 9–14. [CrossRef]

32. Carpenter, J.; Bithell, J. Bootstrap confidence intervals: When, which, what? A practical guide for medical statisticians. *Statist. Med.* **2000**, *19*, 1141–1164. [CrossRef]
33. Gentle, J.E. *Computational Statistics*; Springer: Berlin/Heidelberg, Germany, 2009.
34. Chernick, M.R. *Bootstrap Methods: A Guide for Practitioners and Researchers*, 2nd ed.; Wiley-Interscience: Hoboken, NJ, USA, 2008; ISBN 9780471756217.
35. Lobera, M.P.; Téllez, C.; Herguido, J.; Menéndez, M. Transient kinetic modelling of propane dehydrogenation over a Pt–Sn–K/Al_2O_3 catalyst. *Appl. Catal. A* **2008**, *349*, 156–164. [CrossRef]
36. Aguayo, A.T.; Gayubo, A.G.; Atutxa, A.; Olazar, M.; Bilbao, J. Regeneration of a catalyst based on a SAPO-34 used in the transformation of methanol into olefins. *J. Chem. Technol. Biotechnol.* **1999**, *74*, 1082–1088. [CrossRef]
37. Kern, C.; Jess, A. Regeneration of coked catalysts—Modelling and verification of coke burn-off in single particles and fixed bed reactors. *Chem. Eng. Sci.* **2005**, *60*, 4249–4264. [CrossRef]
38. Sørensen, M.D.P. The establishment of a coke-burn kinetic model for zeolite catalysts. *Chem. Eng. Sci.* **2017**, *168*, 465–479. [CrossRef]
39. Kelling, R.; Kolios, G.; Tellaeche, C.; Wegerle, U.; Zahn, V.M.; Seidel-Morgenstern, A. Development of a control concept for catalyst regeneration by coke combustion. *Chem. Eng. Sci.* **2012**, *83*, 138–148. [CrossRef]
40. Jiang, B.; Zhou, B.; Jiang, Y.; Feng, X.; Liao, Z.; Huang, Z.; Wang, J.; Yang, Y. Kinetic and regenerator modeling of the coke combustion in the moving bed MTP process. *Chem. Eng. Res. Des.* **2017**, *122*, 52–62. [CrossRef]
41. Royo, C.; Perdices, J.M.; Monzón, A.; Santamaría, J. Regeneration of Fixed-Bed Catalytic Reactors Deactivated by Coke: Influence of Operating Conditions and of Different Pretreatments of the Coke Deposits. *Ind. Eng. Chem. Res.* **1996**, *35*, 1813–1823. [CrossRef]
42. Luo, S.; He, S.; Li, X.; Li, J.; Bi, W.; Sun, C. Combustion kinetics of the coke on deactivated dehydrogenation catalysts. *Fuel Process. Technol.* **2015**, *129*, 156–161. [CrossRef]
43. Steen, H. *Handbuch des Explosionsschutzes*; Wiley-VCH: Weinheim, Germany, 2009; ISBN 3527624996.
44. Lin, C.C.; Park, S.W.; Hatcher, W.J. Zeolite catalyst deactivation by coking. *Ind. Eng. Chem. Proc. Des. Dev.* **1983**, *22*, 609–614. [CrossRef]
45. Dumez, F.J.; Froment, G.F. Dehydrogenation of 1-Butene into Butadiene. Kinetics, Catalyst Coking, and Reactor Design. *Ind. Eng. Chem. Proc. Des. Dev.* **1976**, *15*, 291–301. [CrossRef]